3. Sun, L., Berndt, C.C., Gross, K.A., and Kucuk, A. Material fundamentals and clinical performance of plasmasprayed hydroxyapatite coatings: a review. J Biomed Mater Res **58,** 570, 2001.
4. Younger, E.M., and Chapman, M.W. Morbidity at bone graft donor sites. J Orthop Trauma **3,** 192, 1989.
5. Misch, C.E., and Dietsh, F. Bone-grafting materials in implant dentistry. Implant Dent **2,** 158, 1993.
6. Petite, H., Viateau, V., Bensaid, W., Meunier, A., de Pollak, C., and Bourguignon, C. Tissue-engineered bone regeneration. Nat Biotech **18,** 959, 2000.
7. Langer, R., and Vacanti, J.P. Tissue engineering. Science **260,** 920, 1993.
8. Lanza, R.P., Langer, R, and Vacanti, J.P. Principles of Tissue Engineering, second edition. San Diego, CA: Academic Press, 2000.
9. Yamada, Y., Ueda, M., Naiki, T., Takahashi, M., Hata, K., and Nagasaka, T. Autogenous injectable bone for regeneration with mesenchymal stem cells (MSCs) and platelet-rich plasma (PRP)–Tissue-engineered bone regeneration. Tissue Eng **10,** 955, 2004.
10. Yamada, Y., Ueda, M., Naiki, T., and Nagasaka, T. Tissue-engineered injectable bone regeneration for osseointegrated dental implants. Clin Oral Implant Res **15,** 589, 2004.
11. Yamada, Y., Ueda, M., Hibi, H., and Nagasaka, T. Translational research for injectable tissue-engineered bone regeneration using mesenchymal stem cells and platelet-rich plasma—from basic research to clinical case study. Cell Transplant **13,** 343, 2004.
12. Yamada, Y., Ueda, M., Hibi, H., and Baba, S. A novel approach to periodontal tissue regeneration with mesenchymal stem cells and platelet-rich plasma using tissue engineering technology: a clinical case report. Int J Periodontics Restorative Dent **26,** 363, 2006.
13. Yamada, Y., Nakamura, S., Ito, K., Kohgo, T., Hibi, H., Nagasaka, T., and Ueda, M. Injectable tissue-engineered bone using autogenous bone marrow-derived stromal cells for maxillary sinus augmentation: clinical application report from a 2–6-year follow-up. Tissue Eng Part A **14,** 1699, 2008.
14. Marx, R.E., Carlson, E.R., Eichstaedt, R.M., Schimmele, S.R., Stauss, J.E., and Georgeff, K.R. Platelet-rich plasma, growth factor enhancement for bone grafts. Oral Surg Oral Med Oral Path **85,** 638, 1998.
15. Horwitz, E.M., Gordon, P.L., and Koo, W.K. Isolated boned marrow-derived mesenchymal cells engraft and stimulate growth in children with osteogenesis imperfect: implications for cell therapy of bone. Proc Natl Acad Sci USA **99,** 8932, 2002.
16. Kern, S., Eichler, H., Stoeve, J., Klüter, H., and Bieback, K. Comparative analysis of mesenchymal stem cells from bone marrow, umbilical cord blood, or adipose tissue. Stem Cells **24,** 1294, 2006.
17. Pierdomenico, L., Bonsi, L., Calvitti, M., Rondelli, D., Arpinati, M., Chirumbolo, G., Becchetti, E., Marchionni, C., Alviano, F., Fossati, V., Staffolani, N., Franchina, M., Grossi, A., and Bagnara, G.P. Multipotent mesenchymal stem cells with immunosuppressive activity can be easily isolated from dental pulp. Transplantation **80,** 836, 2005.
18. Akintoye, S.O., Lam, T., Shi, S., Brahim, J., Collins, M.T., and Robey, P.G. Skeletal site-specific characterization of orofacial and iliac crest human bone marrow stromal cells in same individuals. Bone **38,** 758, 2006.
19. Yamada, Y., Fujimoto, A., Ito, A., Yoshimi, R., and Ueda, M. Cluster analysis and gene expression profiles: a cDNA microarray system-based comparison between human dental pulp stem cells (hDPSCs) and human mesenchymal stem cells (hMSCs) for tissue engineering cell therapy. Biomaterials **27,** 3766, 2006.
20. Gronthos, S., Mankani, M., Brahim, J., Robey, P.G., and Shi, S. Postnatal human dental pulp stem cells (DPSCs) *in vitro* and *in vivo*. Proc Natl Acad Sci USA **97,** 13625, 2000.
21. Nakamura, S., Yamada, Y., Katagiri, W., Sugito, T., Ito, K., and Ueda, M. Stem cell proliferation pathways comparison between human exfoliated deciduous teeth (SHED) and dental pulp stem cells (DPSCs) by gene expression profile from promising dental pulp. J Endod **35,** 1536, 2009.
22. Miura, M., Gronthos, S., Zhao, M., Lu, B., Fisher, L.W., Robey, P.G., and Shi, S. SHED: stem cells from human exfoliated deciduous teeth. Proc Natl Acad Sci USA **100,** 5807, 2003.
23. Gibson, U.E.M., Heid, C.A., and Williams, A. A novel method for real time quantitative RT-PCR. Genome Res **6,** 995, 1996.
24. Heid, C.A., Stevens, J., and Williams, P.M. Real time quantitative PCR. Genome Res **6,** 986, 1996.
25. Graziano, A., d'Aquino, R., Laino, G., and Papaccio, G. Dental pulp stem cells: a promising tool for bone regeneration. Stem Cell Rev **4,** 21, 2008.
26. Seo, B.M., Sonoyama, W., Yamaza, T., Coppe, C., Kikuiri, T., Akiyama, K., Lee, J.S., and Shi, S. SHED repair critical-size calvarial defects in mice. Oral Dis **14,** 428, 2008.
27. Komori, T., Yagi, H., Nomura, S., Yamaguchi, A., Sasaki, K., Deguchi, K., Shimizu, Y., Bronson, R.T., Gao, Y.H., Inada, M., Sato, M., Okamoto, R., Kitamura, Y., Yoshiki, S., and Kishimoto, T. Targeted disruption of Cbfa1 results in a complete lack of bone formation owing to maturational arrest of osteoblasts. Cell **89,** 755, 1997.
28. Ducy, P., Zhang, R., Geoffroy, V., Ridall, A.L., and Karsenty, G. Osf2/Cbfa1: a transcriptional activator of osteoblast differentiation. Cell **89,** 747, 1997.
29. Schneider, G.B., Zaharias, R., Seabold, D., Keller, J., and Stanford, C. Differentiation of preosteoblasts is affected by implant surface microtopographies. J Biomed Mater Res A **69,** 462, 2004.
30. Berglundh, T., and Lindhe, J. Healing around implants placed in bone defects treated with Bio-Oss. An experimental study in the dog. Clin Oral Implant Res **8,** 117, 1997.
31. Soslau, G., Morgan, D.A., Jaffe, J.S., Brodsky, I., and Wang, Y. Cytokine mRNA expression in human platelets and a megakaryocytic cell line and cytokine modulation of platelet function. Cytokine **9,** 405, 1997.

Address correspondence to:
Yoichi Yamada, D.D.S., Ph.D.
Center for Genetic and Regenerative Medicine
Nagoya University School of Medicine
65 Tsuruma-cho, Showa-ku
Nagoya, Aichi 466-8550
Japan

E-mail: yyamada@.med.nagoya-u.ac.jp

Received: November 13, 2009
Accepted: January 11, 2010
Online Publication Date: March 1, 2010

TISSUE ENGINEERING: Part C
Volume 17, Number 8, 2011

DOI: 10.1089/ten.tec.2011.0003

Viable Cryopreserving Tissue-Engineered Cell-Biomaterial for Cell Banking Therapy in an Effective Cryoprotectant

Eri Umemura, D.D.S.,[1] Yoichi Yamada, D.D.S., Ph.D.,[1] Sayaka Nakamura, D.D.S., Ph.D.,[1] Kenji Ito, D.D.S., Ph.D.,[2] Kenji Hara, D.D.S.,[2] and Minoru Ueda, Ph.D.[1]

The application of cell-biomaterial systems in tissue engineering and regenerative medicine is an important challenge in biomedicine, which preserves not only cells, but also tissue-engineered constructs. In this study, the constructs and cryoprotectant parameters were optimized, and it was evaluated whether the characteristics of dental pulp stem cells (DPSCs), which have high proliferation ability as stem cells, were maintained during encapsulation and cryopreservation. The optimal cell-biomaterial gel constructs with the gelation rate of 2% alginate: 100 mM $CaCO_3$: 200 mM glucono-δ-lactone (GDL) = 4:1:1 and suitable cryoprotectants (CPAs) used for cryopreservation were Dulbecco's modified Eagle's medium (DMEM) supplemented with 10% ethylene glycol (EG), 1.0 M sucrose and 0.00075 M polyvinylpyrrolidone (PVP). Optimality was confirmed by cell viability (trypan blue, live/dead analysis), the proliferation of DPSCs, and the microstructure using scanning electron microscopy (SEM) in the constructs, and surface epitope by flow cytometric analysis before and after cryopreservation. There were no visible differences in the structure. In conclusion, this study indicates that the optimal cell-biomaterial gel constructs and the cryoprotectant are promising biomaterials. The defined encapsulation/thawing system offers an excellent option for cell-banking therapy to be developed with ready-to-use viable biomaterials and patient-specific products as drug delivery systems.

Introduction

TISSUE ENGINEERING and regenerative medicine (TERM) has been recognized as a promising method to restore damaged tissues and maintain biological functions.[1,2] Among the therapies used in TERM, cell-based therapies have been one of the recent highlights. These therapies have been noted to regenerate lost tissues and provide a sustained source of many beneficial factors. In particular, stem cells seeded in scaffolds are used to enable cell function adaptation by stem cells[3] Numerous studies have also been developed with the goal of producing clinically useful scaffolds (e.g., scaffold design and material selection).[3–5] Further, challenges in scaffold fabrication are to encapsulate cells into scaffolds to create synthesis/living composite biomaterials; however, the process of sourcing, growing, and encapsulation is labor intensive and difficult to apply for acute diseases. As a result of this limitation, an attractive system to cryopreserve the cell-biomaterial construct has emerged.[6–8]

The biomaterials used as scaffolds are natural or synthetic polymers such as polysaccharides, hydrogels, or thermoplastic elastomers. In particular, hydrogel provides a three-dimensional environment similar to that *in vivo* and, therefore, allows cells to maintain their characteristics and function well in the body. The hydrogels used most frequently in TERM are agarose, alginate, collagen, fibrin, gelatin, and hyaluronic acid. Among these, the sources of collagen, fibrin, and gelatin are animal/human proteins; and the source of hyaluronic acid is animal/human polysaccharide, but the source of agarose and alginate is seaweed. The alginate gelation method uses ionotrophic cross linking and is degradable by ion exchange, whereas the agarose gelation method uses thermal change and is nondegradable.[9] In this study, alginate, known for its safe, low-cost, biodegradable, and easy-to-manipulate properties, was examined as a scaffold.

The role of cryoprotectants (CPAs) is to replace water in cells/tissue and to form an amorphous state at low temperature. Ideal CPAs can be achieved using penetrating cryoprotectants with the additional usage of nonpenetrating cryoprotectants.[10] The problem with conventional CPAs is that they contain dimethyl sulfoxide (DMSO) and animal substances. DMSO has long been used as a cryoprotectant for its high penetrating property; however, due to its cytotoxicity, an alternative agent is required. Serum or protein additives have also been used in CPAs to protect cells, but the possibility of contamination remained.[11–14] CPAs that do

[1]Department of Oral and Maxillofacial Surgery, Nagoya University Graduate School of Medicine, Nagoya, Japan.
[2]Hamamatsu Kita Hospital, Shizuoka, Japan.

not contain DMSO or protein additives need to be developed but are highly expensive.

Next, as a cell source of important TERM elements, we focused on dental pulp stem cells (DPSCs), which have high proliferation and differentiation ability and have been considered appropriate candidates not only for dental tissue regeneration but also for the treatment of general diseases.[15–18] We encapsulated the DPSCs in alginate gel and optimized the gelation rate containing $CaCO_3$ and glucono-δ-lactone (GDL).[19] After fabricating the cell-biomaterial constructs, we cryopreserved them in CPAs. For medical approval, we examined the optimized condition of ethylene glycol (EG) as a penetrating cryoprotectant and sucrose and polyvinylpyrrolidone (PVP) as nonpenetrating cryoprotectants without DMSO and animal substances. EG, sucrose, and PVP have the merit of being cost-effective CPAs.

Taken together, the approach in this study contributes to the development of effective cryopreservation methods and novel cell banking therapy with ready-to-use viable biomaterials, which reduce the time to fabricate cell-biomaterial constructs and are easy packaging treatments in tissue engineering and medicine technology.

Materials and Methods

Culture of DPSCs and formation of the cell-biomaterial gel encapsulation

Isolation and culture of DPSCs. Human dental pulp tissues were obtained from clinically healthy extracted deciduous teeth. The experimental protocols were approved by the ethics committee of Nagoya University. DPSCs were isolated and cultured as previously described.[15,17] Briefly, the pulp was gently removed and digested in a solution of 3 mg/mL collagenase type I and 4 mg/mL dispase for 1 h at 37°C. After filtration using 70-mm cell strainers (Falcon; BD Labware, Franklin Lakes, NJ), cells were cultured in Dulbecco's modified Eagle's medium (DMEM) (GIBCO, Rockville, MD) containing 20% mesenchymal cell growth supplement (Lonza, Inc., Walkersville, MD) and antibiotics (100 U/mL penicillin, 100 μg/mL streptomycin, and 0.25 μg/

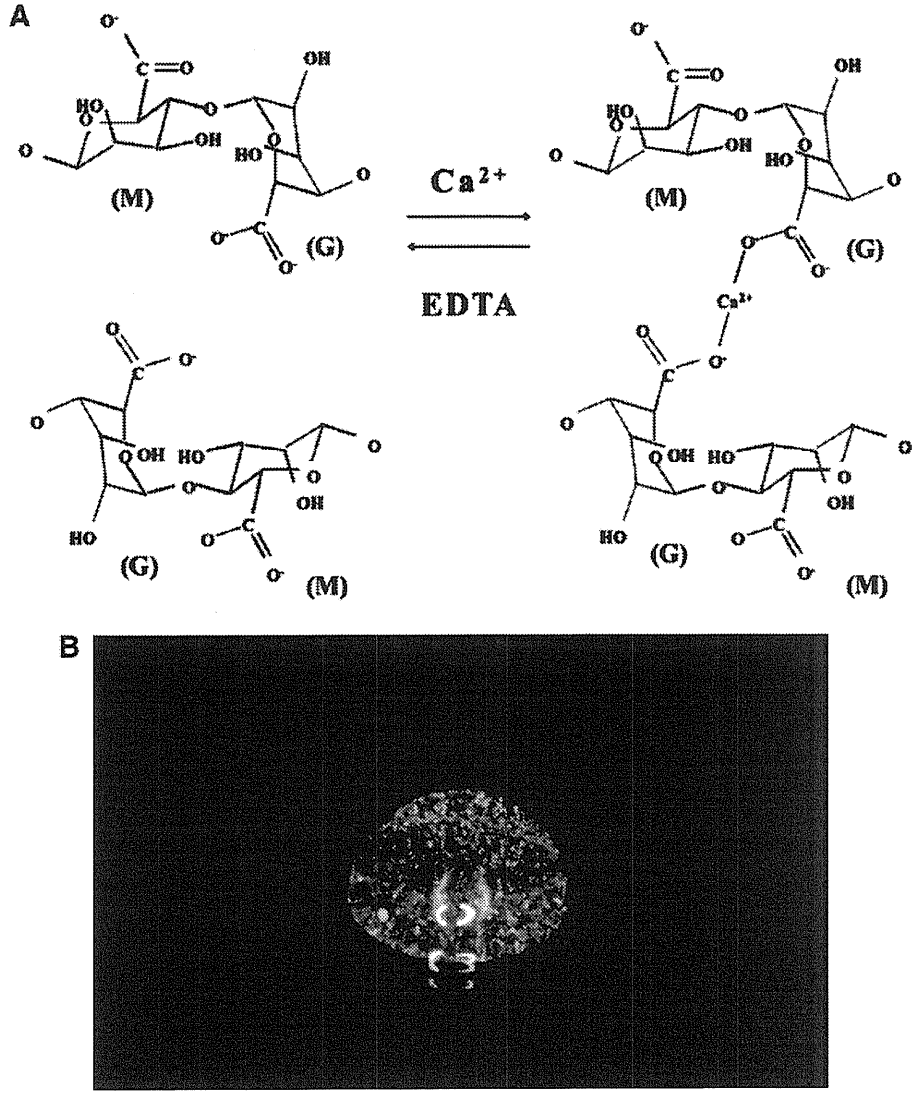

FIG. 1. **(A)** Alginate polysaccharide consisting of one α-L-guluronic acid (G) and one β-D-mannuronic (M) residue with (1,4)-linkages. G-block regions can dimerize to form hydrogels in the presence of aqueous divalent cations, such as calcium. **(B)** Macro view of cell-biomaterial gel construct formation.

mL amphotericin B; GIBCO) at 37°C under 5% CO_2. After primary culture, cells were subcultured at about 1×10^4 cells/cm^2. The cells were used in the experiment from one to five passages.

Optimization of cell encapsulation with alginate gel (cell-biomaterial gel constructs). DPSCs were encapsulated in alginate gel, the gelation rate of which was controlled using $CaCO_3$ (Sigma-Aldrich, Tokyo, Japan) and GDL (Sigma-Aldrich, St Louis, MO). The $CaCO_3$ to GDL molar ratio of 0.5 was maintained to achieve a neutral pH. The DPSCs were mixed with the 5 w/v sodium alginate solution (Kaigen, Hokkaido, Japan) to obtain a final density of 5.0×10^6 cells/mL before the gelation process. Cell-biomaterial gel constructs were fabricated by pipetting $CaCO_3$ solution and GDL solution into the cell-alginate solution (Fig. 1). The gelation rate of experimental groups was as follows: 2% alginate: 100 mM $CaCO_3$: 200 mM GDL: (1) 1:1:1, (2) 2:1:1, (3) 3:1:1, (4) 4:1:1, (5) 5:1:1, (6) 6:1:1, respectively, and the formation and viability of the encapsulated DPSCs were investigated. The average gel diameter was 5 mm. After fabrication, cell-biomaterial gel constructs were cultured for up to 7 days at 37°C under 5% CO_2.

Cryopreservation

Optimization of CPAs. The optimal CPAs were determined by investigating CAPs of various mixture rates (Fig. 2). The agents tested were (1) DMEM + 10% EG (Wako, Osaka, Japan), (2) DMEM + 10% EG + 1.0 M sucrose (Wako), (3) DMEM + 10% EG + 1.0 M sucrose + 0.00025 M PVP (Sigma-Aldrich, St. Louis, MO), (4) DMEM + 10% EG + 1.0 M sucrose + 0.0005 M PVP, (5) DMEM + 10% EG + 1.0 M sucrose + 0.00075 M PVP, (6) DMEM + 40% EG + 0.6 M sucrose, (7) DMEM + 10% fetal bovine serum (FBS) + 12% DMSO (Wako), and (8) Banbanker (Genetics, Tokyo, Japan). Among these agents, the most optimal CPAs were determined by

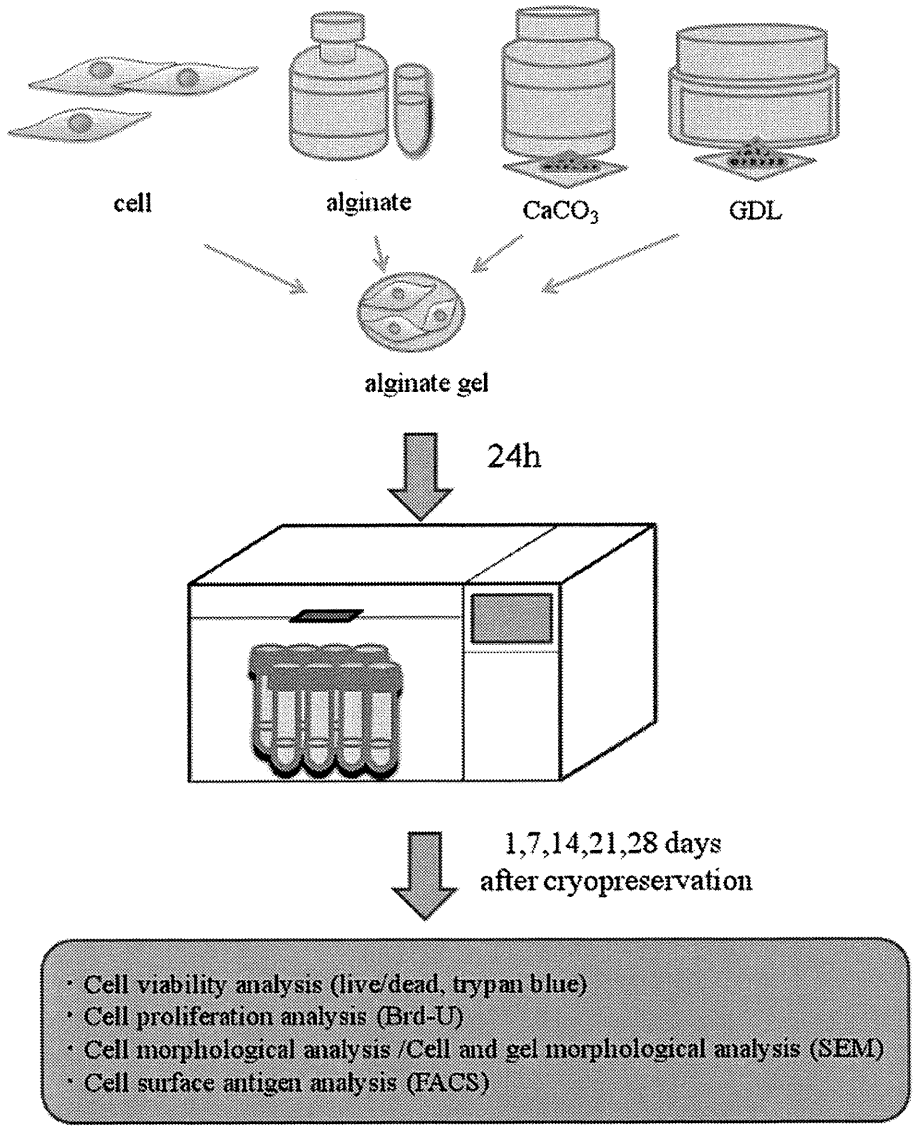

FIG. 2. Schematic illustration of the preparation of cell-biomaterial gel constructs and experimental protocol.

cell viability. All materials used in this study were analytical grade.

Cryopreservation procedures and subsequent culture of cell-biomaterial gel constructs. Cell-biomaterial gel constructs were divided into two groups: (1) control: cell-biomaterial gel constructs without undergoing cryopreservation-thawing process; (2) cryopreservation: cell-biomaterial gel constructs treated with cryopreservation-thawing process. The cell-biomaterial gel constructs were cultured for 24 h at 37°C under 5% CO_2, and then 1 gel was added to each 1.8 mL cryotube (Nunc, Rochester, NY). For the cryopreservation process, cell-biomaterial gel constructs were left at 4°C for 5 min, −30°C for 30 min, and finally stored at −80°C for 1, 7, 14, 21, and 28 days. For the warming process, cell-biomaterial gel constructs were thawed directly in a water bath at 37°C. The cell-biomaterial gel constructs were lysed using 0.5 M ethylene diamine tetraacetic acid (EDTA) (Gibco, Auckland, NZ), and the resulting cell suspension was cultured at 37°C under 5% CO_2 or was analyzed without it. The cells were cultured for 7 days after thawing and before analyzing.

Analysis of cell viability with trypan blue and live/dead assay

Cells in the gel suspension were stained with 0.4% trypan blue (Invitrogen, Tokyo, Japan) to investigate the dead cells. The number of surviving and dead cells was counted, and the survival rate was calculated using Vi-CELL XR (Beckman Coulter, Tokyo, Japan). Noncryopreserved cell-biomaterial gel suspension was used as a control. The cell viability of cell-biomaterial gel constructs in both control and cryopreserved groups was also assayed by confocal laser microscopy using the LIVE/DEAD Viability/Cytotoxicity Kit (Invitrogen, Eugene, OR). Images were obtained with a Nikon confocal razor microscope A1Rsi (Nikon, Tokyo, Japan) with excitation wavelengths of 488 nm and 543 nm for calcein-AM and ethidium homodimer, respectively. Z stacks of images composed of 17–24 optical slices with z axis steps of 5 μm were obtained for each cell-biomaterial gel construct, and maximum projection images were made with the aid of NIS-Elements AR 3.0 software.

Analysis of cell proliferation

The proliferation rates of cultured DPSCs in cell-biomaterial gel construct suspensions of both control and cryopreserved groups were assessed by bromodeoxyuridine (BrdU) incorporation for 24 h using a BrdU staining kit according to the manufacturer's instructions (Invitrogen, Carlsbad, CA).

Assessment of microstructure using scanning electron microscopy

Cell-biomaterial gel constructs from both control and cryopreserved groups were rinsed three times with phosphate-buffered saline (PBS) and fixed in 10% formalin solution (Wako) for 30 min. The constructs were dehydrated with an increasing gradient of ethanol solutions (70%, 80%, 90%, 95%, and 100%), treated with t-butyl alcohol, and freeze dried with liquid nitrogen. Each sample was mounted, sputter-coated with osmium, and examined using scanning electron microscopy (SEM; JEOL JSM-7600; JEOL Ltd, Tokyo, Japan) with 2 kV accelerating voltage.

Analysis of surface epitope by flow cytometric analysis

Cultured DPSCs from both control and cryopreserved groups were analyzed by flow cytometric analysis according to a previous method.[20] Fluorescein isothiocyanate (FITC)-conjugated mouse antibodies against human CD13, CD14, CD29, CD31, CD34, biotin-conjugated mouse antibody against human CD44, CD45, CD73, CD146 (BD Biosciences, San Jose, CA), and CD105 (Ancell Corporation, Bayport, MN) were used for analysis of specific surface antigens. PerCP-conjugated streptavidin (BD Biosciences) was used as

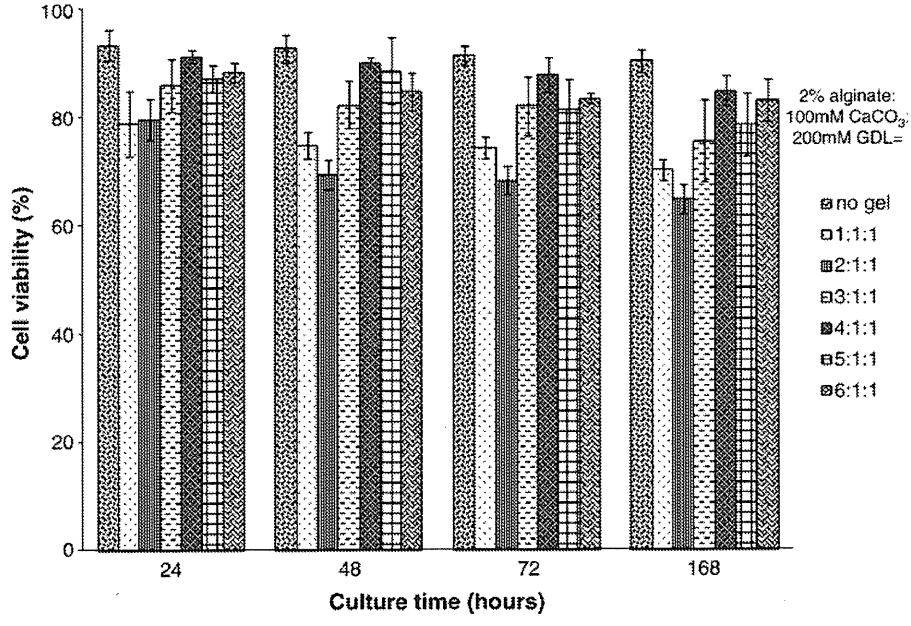

FIG. 3. Cell viability at different gelation rates of cell-biomaterial gel constructs using 2% alginate solution, $CaCO_3$ solution, and GDL solution after culture (h). Bar: standard deviation ($n = 3$). GDL, glucono-δ-lactone.

the secondary antibody to detect biotin-conjugated mouse antibody against human CD44.

Statistical analysis

Statistical differences were evaluated using the Tukey-Kramer test after one-way analysis of variance. $p < 0.05$ was considered significant.

Results

Optimization of cell-biomaterial gel constructs

The optimal gel constructs were determined by the homogeneity of the gel and the viability of the encapsulated cells. The gelation rate of the alginate gels that would be easy to manipulate was investigated (Fig. 1). Homogenous alginate gels were investigated by controlling the gelation rate to 2% alginate: 100 mM $CaCO_3$: 200 mM GDL = 1–6: 1:1. At a rate higher than 5:1:1, full gelation did not occur, and the gel obtained was not homogeneous with the rate lower than 1:1:1. Next, the optimal gelation rate was investigated by analyzing the survival rate of DPSCs cultured in the gels. The optimal cell-biomaterial gel constructs were determined with a gelation rate of 2% alginate: 100 mM $CaCO_3$: 200 mM GDL = 4:1:1 (Fig. 3). The percentage of surviving cells at a gelation rate of 4:1:1 was 92.3 ± 5.4, 90.9 ± 6.2, 85.3 ± 5.5, and 82.5 ± 5.4 at 24, 48, 72, and 168 h, respectively (Fig. 3). Cell survival at this gelation rate showed statistically significant differences between 4:1:1 and 1:1:1 or 2:1:1 at 24, 48, 72, and 168 h; between 5:1:1 and 1, 2, 3:1:1, or between 6:1:1 and 2:1:1 or between 3:1:1 and 2:1:1 at 48 h; between 6:1:1 and 1, 2, 3:1:1 at 72 h; or 5, 6:1:1 and 2:1:1 at 168 h. However, there were no significant differences between 4, 5, 6:1:1 and the positive control (only the cells without gelation) at all times (Fig. 3).

Optimization of CPAs

The optimal CPAs were determined by the survival rate of cells (trypan blue staining, live/dead analysis) after the cryopreservation-thawing process. CPAs containing EG,

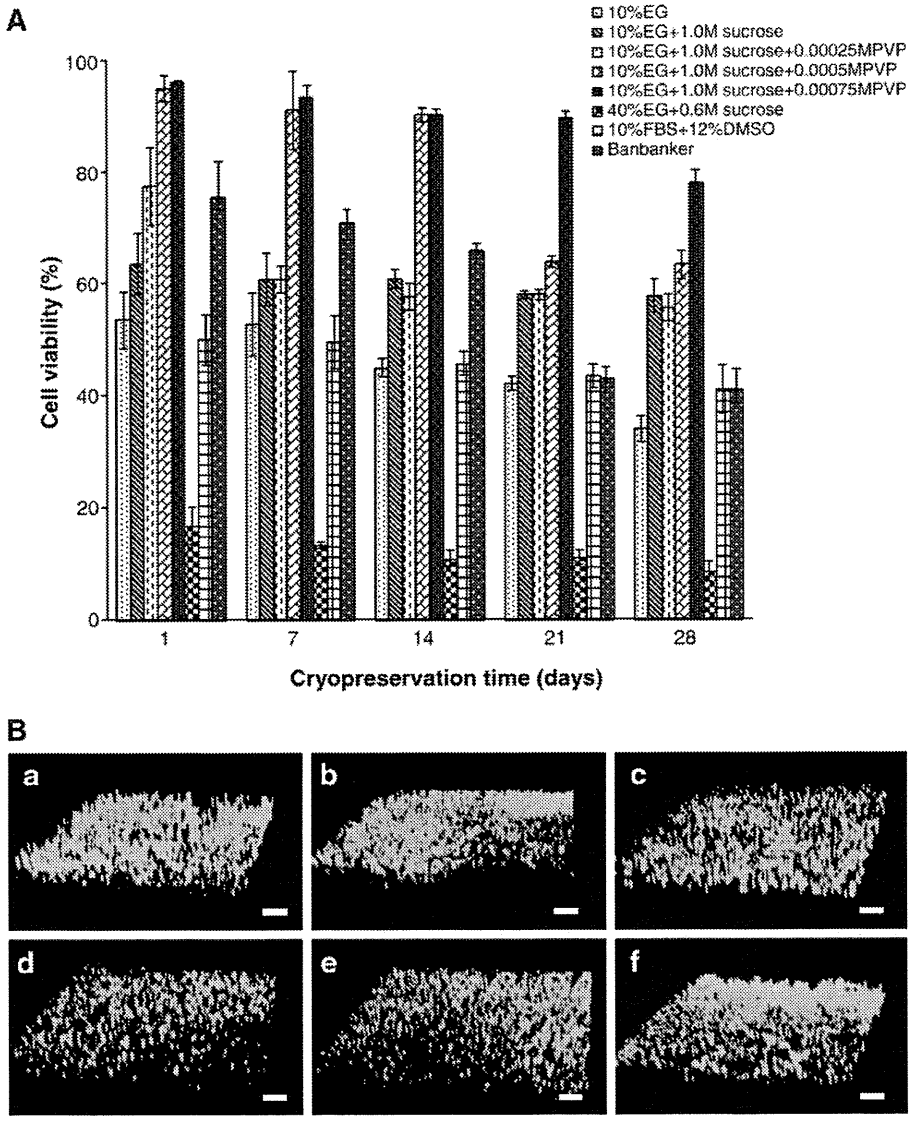

FIG. 4. **(A)** Cell viability after 1, 7, 14, 21, and 28 days of cryopreservation. Bar: standard deviation ($n = 3$). **(B)** Confocal lazer scanning microscopy images of control (noncryopreserved) and cryopreserved groups. Viability of encapsulated DPSCs at different time points, **(a)** control, and cryopreservation at 1 day **(b)**, 7 days **(c)**, 14 days **(d)**, 21 days **(e)**, and 28 days **(f)**. Viable cells stained green with ethidium homodimer, whereas nonviable cells stained red with calcein-AM. DPSC, dental pulp stem cell.

sucrose, and PVP were revealed to have better cell viability than the existing commercial product (Banbanker). Further analysis was performed by controlling the mixture rate of EG, sucrose, and PVP. The percentage of surviving cells (cell viability) using CPAs containing DMEM + 10% EG + 1.0 M sucrose + 0.00075 M PVP group was 92.1 ± 3.4, 91.8 ± 1.4, 90.3 ± 0.9, 89.4 ± 1.3, and 77.8 ± 2.5 at 1, 7, 14, 21, and 28 days, respectively. The cell viability of CPAs showed statistically significant differences between DMEM + 10% EG + 1.0 M sucrose + 0.00075 M PVP group and DMEM + 10% EG group, DMEM + 10% EG + 1.0 M sucrose group, DMEM + 10% EG + 1.0 M sucrose + 0.00025 M PVP group, DMEM + 40% EG + 0.6 M sucrose group, DMEM + 10% FBS + 12% DMSO group, and Banbanker group at 1, 7, and 14 days, and all groups at 21 and 28 days; therefore, DMEM supplemented with 10% EG, 1.0 M sucrose, and 0.00075 M PVP was the most optimal CPA (Fig. 4). There were no significant differences among these days, and they corresponded with the data from trypan blue staining.

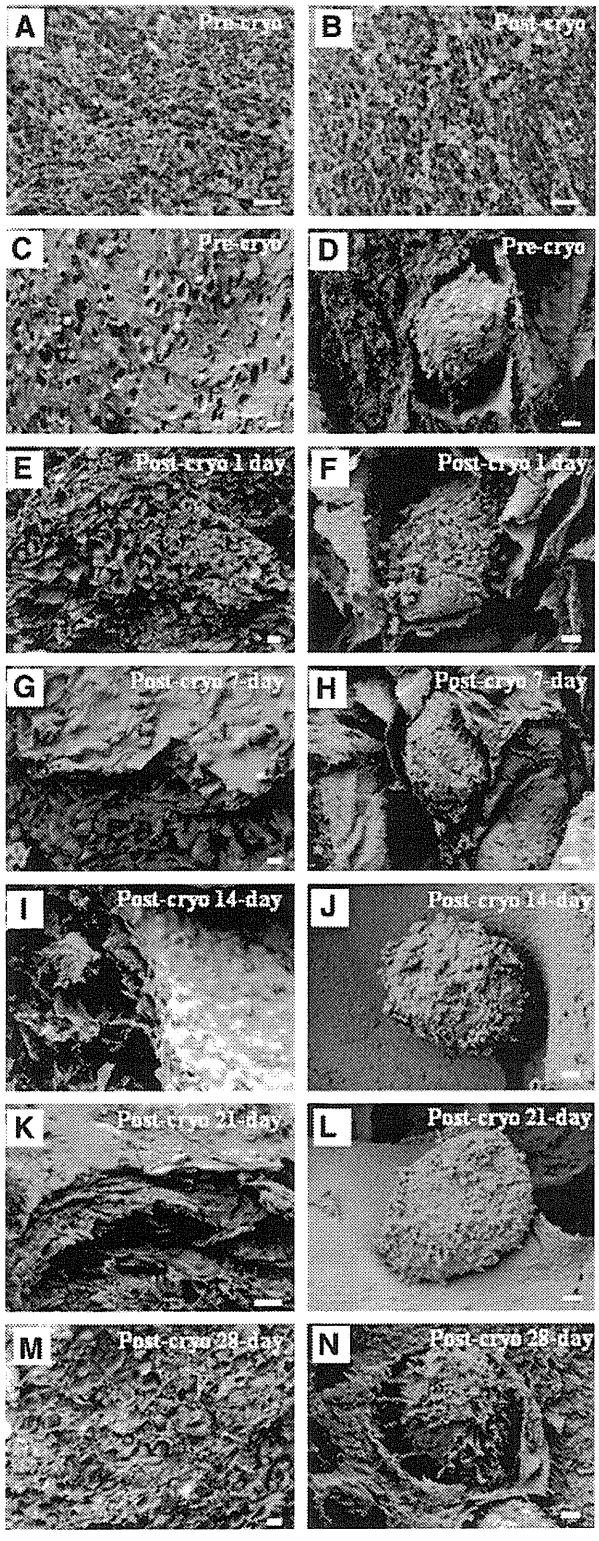

Characterization of DPSCs before and after cryopreservation-thawing process

Microstructure of the cell-biomaterial gel constructs after thawing process by SEM images. In the thawing process, the microstructure of cell-biomaterial gel constructs with and without cells (DPSCs) was examined. Low-magnification SEM images before and after cryopreservation showed no visible differences in the structure (Fig. 5A, B). Even at low magnification, DPSCs were found in cell-biomaterial gel constructs before cryopreservation and after 1, 7, 14, 21, and 28 days (Fig. 5C, E, G, I, K, M). The pore structures of the constructs were retained. At higher magnification, the cell morphology was intact in the constructs with no differences (Fig. 5D, F, H, J, L, N). Representative images revealed that the integrity of constructs was maintained during the process (cooling and warming), and the cells survived.

Effects of DPSCs proliferation ability and cell-surface antigen in the constructs on cryopreservation time. The proliferation rate of DPSCs cultured in the optimized cell-biomaterial gel constructs in both control and cryopreserved groups was assessed using BrdU staining. The percentage of BrdU-positive cells in control and cryopreserved groups at 1, 7, 14, 21, and 28 days was 82.0 ± 5.0, 80.7 ± 3.9, 78.2 ± 6.3, 77.8 ± 2.1, 76.2 ± 4.0, and 76.0 ± 6.3, respectively (Fig. 6A). DPSCs proliferation showed no significant difference between control and cryopreservation groups. Consequently, there was no cryopreservation impact on cell proliferation.

We have previously confirmed that DPSCs exhibit the characteristics of mesenchymal stem cells (MSCs).[18,20] In the present study, the expression pattern of DPSCs was

FIG. 5. Scanning electron microscopy images of alginate and cell-biomaterial gel constructs showing the impact of cryopreservation. Sections of alginate gels without cells: precryopreserved constructs **(A)**, cryopreserved constructs **(B)**. Sections of cell-biomaterial gel constructs: pre-cryopreserved constructs **(C, D)**, cryopreserved constructs 1 **(E, F)**, 7 **(G, H)**, 14 **(I, J)**, 21 **(K, L)**, and 28 **(M, N)** days after thawing process. Wide view images **(A, B, C, E, G, I, K, M)** show structure integrity, magnified cells **(D, F, H, J, L, N)** illustrate clear view of microstructure. Scale bars represent 10 μm **(A, B, C, E, G, I, K, M)**, 1 μm **(D, F, H, J, L, N)**, respectively. pre-cryo, precryopreservation; post-cryo, post-cryopreservation.

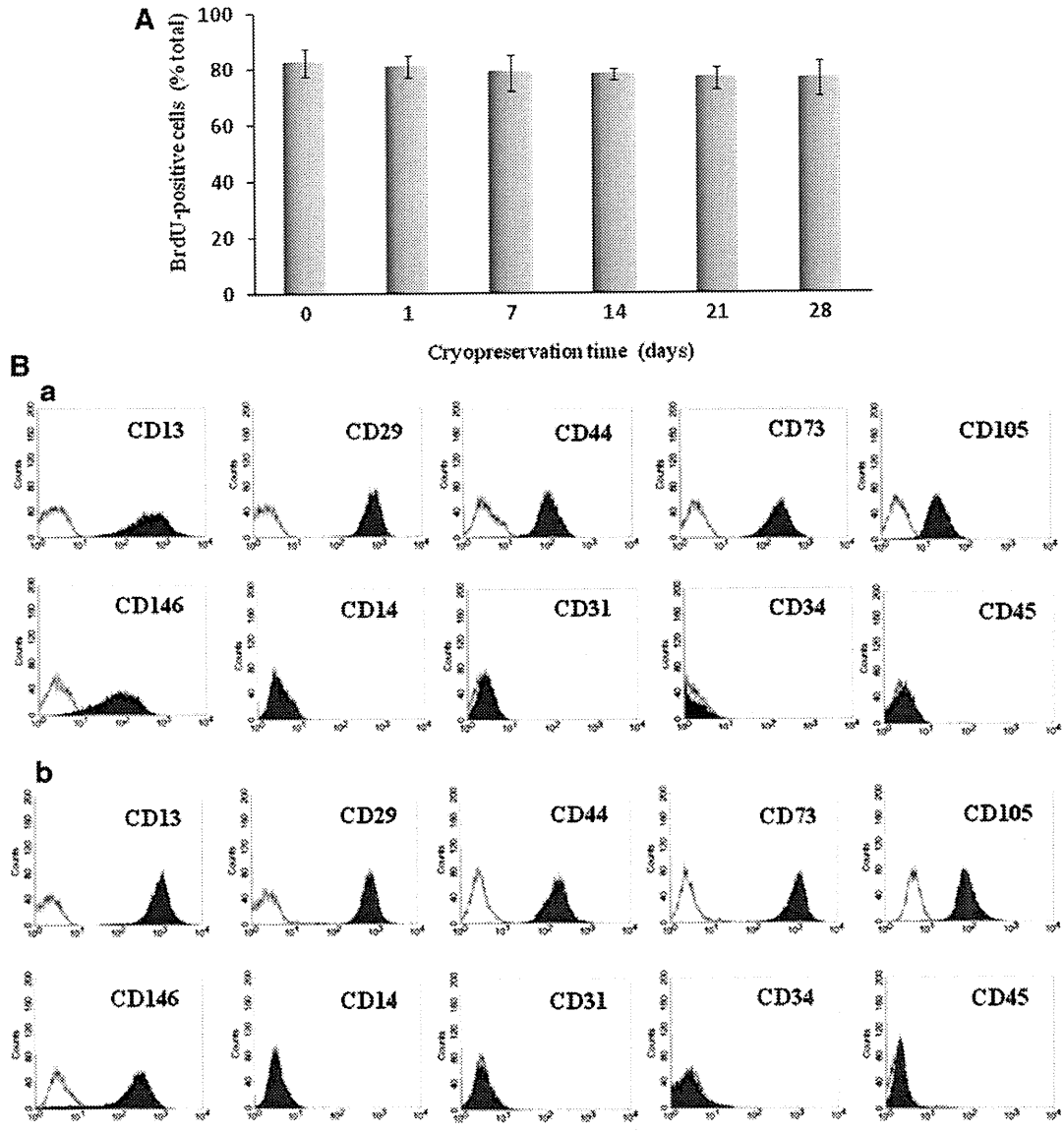

FIG. 6. **(A)** Cell proliferation rates of control and cryopreserved groups (1, 7, 14, 21, and 28 days after cryopreservation-warming process) were assessed using BrdU. Bar: standard deviation ($n=3$). **(B)** Typical flow cytometric analysis diagrams on the expression of MSC markers CD13, CD29, CD44, CD73, CD105, and CD146, as well as hematopoietic markers CD34, and CD45, and monocytic markers CD14, CD31. **(a)** Control and **(b)** cryopreserved group. The cells cryopreserved for 28 days were used in this study. BrdU, bromodeoxyuridine; MSC, meschymal stem cell.

investigated and was found to be comparable to that of MSCs. The expression pattern of DPSCs encapsulated in cell-biomaterial gel constructs and cryopreserved in CPAs was also investigated. It was found that encapsulated and cryopreserved DPSCs also preserved the expression pattern of markers even after cryopreservation (Fig. 6B).

Discussion

Alginate gels are easy to manipulate, and the gels used in this study, which are used clinically to protect cells and tissues, are safe. They were solvated using EDTA as a chelating agent and GDL as a pH reducing agent and formed gels in the presence of aqueous divalent cations, such as Ca^{2+}.[19] The alginate gel with a gelation rate of 2% alginate: 100 mM $CaCO_3$: 200 mM GDL=4:1:1 was found to be optimal by investigating the survival rate of cells cultured in the cell-biomaterial gel constructs (Fig. 3). The viability of the encapsulated cells might have been maintained because of the mild internal environment of the gel.

An ideal CPA is a solution that is nontoxic to cells/tissues even after prolonged exposure. Strategies to avoid toxic effects of the solutions require component selection and adjustment of the solute concentration. This minimizes damage caused by ice formation and encourages the formation of an amorphous state in cells/tissues.[21] Currently, effective CPAs commonly consist of a minimum of two (penetrating cryoprotectant+sugar/polymer) or three (penetrating

cryoprotectant + sugar + polymer) components.[16] The most traditional penetrating cryoprotectants, including DMSO, glycerol, and EG, have been tested alone and in combination.[22] EG is known for its detrimental effects on developmental potential, membrane integrity and cytoskeletal structure, which has made it the principal penetrating cryoprotectant.[22] As a nonpenetrating cryoprotectant, sugar is used as an important component of osmotic buffers. In this study, we used sucrose, a monosaccharide that can be dissolved more efficiently in solutions of penetrating CPAs, than either the disaccharides or polysaccharides. In terms of polymers, we used PVP for its ability to cryopreserve delicate tissues.[23] This is used in a wide variety of applications in medicine, pharmacy, cosmetics, and industrial production and is also known to be a more effective CPA than other polymers, such as dextran and Ficoll.[24] In this study, the cell viability of DPSCs was investigated in various CPAs. The viability of CPAs in DMEM supplemented with 12% DMSO and 10% FBS, commercial CPAs (Banbanker), DMEM supplemented with 10% EG, and 1.0 M sucrose and 0.00075 M PVP, which were the optimized CPAs, was 49.8% ± 4.5%, 77.5% ± 6.5%, and 96.1% ± 0.4% on day 1, respectively (Fig. 4A). No visual difference between the cell viability of control and cryopreserved gel was found when observed through a confocal microscope with trypan blue staining after 1, 7, 14, 21, and 28 days of cryopreservation (Fig. 4B). Moreover, the maintenance of structure integrity is a prerequisite in the cryopreservation of cell-biomaterial constructs, and the cryopreserved constructs were undamaged, such as the cell surface of SEM images showed no significant difference in microstructure between the control and cryopreserved groups (Fig. 5). The cryopreserved structure of the constructs appeared to have more pores and wrinkles on the surface (Fig. 5). This optimized CPA is DMSO, serum, and animal substance free; and the cryopreserved-thawed DPSCs had normal morphology (data not shown), maintained the properties of multipotent cells with high proliferation ability, and expressed the corresponding marker of MSCs (Fig. 6). Therefore, the matricellular environment of the DPSCs in our cell-biomaterial gel and CPAs constructs also remained unaltered. These results imply that the constructs were well preserved during the cooling-warming cycle and the DPSCs would be well protected.

On the other hand, culturing and expanding cells *ex vivo* is lengthy and costly work, and obtaining a sufficient cell number for tissue engineering applications would take some months[25]; therefore, if well-preserved viable cell-biomaterial constructs could be prepared, it would eliminate the lengthy waiting period and bring down the medical fees. An attractive aspect of applying cell-biomaterial gel constructs and their successful long-term storage lies in the potential of providing immediate solutions to patients with acute diseases. Moreover, cell-biomaterial constructs and the application of CPAs are a step toward the application of stem cells such as DPSCs in TERM and provide novel tissue-engineering products, such as ready-to-use and patient-specific products, for cell-based services or drug delivery systems.

Conclusion

In this study, we optimized cell-biomaterial gel constructs and cryoprotectant parameters, and it was found that the characteristics of DPSCs were maintained during encapsulation and cryopreservation. In conclusion, this study indicates that the optimal cell-biomaterial gel constructs and the cryoprotectant could be promising biomaterials. The defined encapsulation/thawing system offers an excellent simple option for cell-banking therapy.

Acknowledgments

The authors are grateful to the members of the Department of Oral and Maxillofacial Surgery, Nagoya University Graduate School of Medicine, for discussions. This work was partly supported by Grants-in-Aid for Scientific Research (Nos. 20659297, 21390507, 21791848) from the Japan Society for the Promotion of Science.

Disclosure Statement

No competing financial interests exist.

References

1. Langer, R., and Vacanti, J.P. Tissue engineering. Science **260,** 920, 1993.
2. Khademhosseini, A., Langer, R., Borenstein, J., and Vacanti, J.P. Microscale technologies for tissue engineering and biology. Proc Natl Acad Sci USA **103,** 2480, 2006.
3. Levenberg, S., Huang, N.F., Lavik, E., Rogers, A.B., Itskovitz-Eldor, J., and Langer, R. Differentiation of human embryonic stem cells on three-dimensional polymer scaffolds. Proc Natl Acad Sci USA **100,** 12741, 2003.
4. Hunt, N.C., Shelton, R.M., and Grover, L.M. Reversible mitotic and metabolic inhibition following the encapsulation of fibroblasts in alginate hydrogels. Biomaterials **30,** 6435, 2009.
5. Yamada, Y., Ueda, M., Naiki, T., Takahashi, M., Hata, K., and Nagasaka, T. Autogenous injectable bone for regeneration with mesenchymal stem cells and platelet-rich plasma: tissue-engineered bone regeneration. Tissue Eng **10,** 955, 2004.
6. Zimmermann, H., Ehrhart, F., Zimmermann, D., Muller, K., Katsen-Globa, A., Behringer, M., Feilen, P.J., Gessner, P., Zimmermann, G., Shirley, S.G., Weber, M.M., Metze, J., and Zimmermann, U. Hydrogel-based encapsulation of biological, functional tissue: fundamentals, technologies and applications. Appl Phys Mater Sci Process **89,** 909, 2007.
7. Bhakta, G., Lee, K.H., Magalhaes, R., Wen, F., Gouk, S.S., Hutmacher, D.W., and Kuleshova, L.L. Cryopreservation of alginate-fibrin beads involving bone marrow derived mesenchymal stromal cells by vitrification. Biomaterials **30,** 336, 2009.
8. Matsumoto, Y., Morinaga, Y., Ujihara, M., Oka, K., and Tanishita, K. Improvement in the viability of cryopreserved cells by microencapsulation JSME. Int J C Mech Syst Machine Elem Manuf **44,** 937, 2001.
9. Hunt, N.C., and Grover, L.M. Cell encapsulation using biopolymer gels for regenerative medicine. Biotechnol Lett **32,** 733, 2010.
10. Kuleshova, L.L., Gouk, S.S., and Hutmacher, D.W. Vitrification as a prospect for cryopreservation of tissue-engineered constructs. Biomaterials **28,** 1585, 2007.
11. Mukaida, T., Wada, S., Takahashi, K., Pedro, P.B., An, T.Z., and Kasai, M. Vitrification of human embryos based on the assessment of suitable conditions for 8-cell mouse embryos. Hum Reprod **13,** 2874, 1998.

TISSUE ENGINEERING: Part A
Volume 17, Numbers 9 and 10, 2011

DOI: 10.1089/ten.tea.2010.0306

Dental Pulp-Derived CD31$^-$/CD146$^-$ Side Population Stem/Progenitor Cells Enhance Recovery of Focal Cerebral Ischemia in Rats

Masahiko Sugiyama, D.D.S.,[1,2] Koichiro Iohara, Ph.D.,[1] Hideaki Wakita, Ph.D.,[3] Hisashi Hattori, Ph.D.,[2] Minoru Ueda, Ph.D.,[2] Kenji Matsushita, Ph.D.,[1] and Misako Nakashima, Ph.D.[1]

Regenerative therapy using stem cells is a promising approach for the treatment of stroke. Recently, we reported that CD31$^-$/CD146$^-$ side population (SP) cells from porcine dental pulp exhibit highly vasculogenic potential in hindlimb ischemia. In this study, we investigated the influence of CD31$^-$/CD146$^-$ SP cells after transient middle cerebral artery occlusion (TMCAO). Adult male Sprague-Dawley rats were subjected to 2 h of TMCAO. Twenty-four hours after TMCAO, CD31$^-$/CD146$^-$ SP cells were transplanted into the brain. Motor function and infarct volume were evaluated. Neurogenesis and vasculogenesis were determined with immunochemical markers, and the levels of neurotrophic factors were assayed with real-time reverse transcription–polymerase chain reaction. In the cell transplantation group, the number of doublecortin-positive cells increased twofold, and the number of NeuN-positive cells increased eightfold, as compared with the control phosphate-buffered saline group. The vascular endothelial growth factor level in the ischemic brain with transplanted cells was 28 times higher than that in the normal brain. In conclusion, CD31$^-$/CD146$^-$ SP cells promoted migration and differentiation of the endogenous neuronal progenitor cells and induced vasculogenesis, and ameliorated ischemic brain injury after TMCAO.

Introduction

Several preclinical studies have provided evidence that transplanted stem cells have therapeutic potential in the treatment of stroke.[1] Stem cells have the capability to migrate to areas of injury and secrete neuroprotective factors to induce neurogenesis.[2] In the adult mammalian brain, neurogenesis persists in certain distinct regions of the central nervous system such as the subventricular zone (SVZ) and the dentate gyrus of the hippocampus.[3] It has been reported that transplanting differentiated neural stem cells isolated from dental pulp improved motor disability and reduced infarct volume.[4] However, the influence of transplanting stem/progenitor cells isolated from dental pulp in cerebral ischemia has not been elucidated. Recently, we reported that CD31$^-$/CD146$^-$ side population (SP) cells containing stem/progenitor cells from porcine dental pulp exhibit highly vasculogenic potential *in vitro* and promote revascularization in hindlimb ischemia.[5] In the present study, we investigated the effects of these cells on neurogenesis and vasculogenesis in a cerebral ischemia model in a rat. In addition, the effects on the motor dysfunction and infarct volume were evaluated after transient middle cerebral artery occlusion (TMCAO).

Materials and Methods

Isolation of CD31$^-$/CD146$^-$ SP cells

CD31$^-$/CD146$^-$ SP and CD31$^+$/CD146$^-$ SP cells were isolated from porcine tooth germ, as described previously.[5] CD31$^-$/CD146$^-$ SP cells were cultured in endothelial basal medium-2 (EBM-2, single quots cc–4176) with 10 ng/mL insulin-like growth factor 1 (IGF1), 10 ng/mL epidermal growth factor (EGF), and 10% fetal bovine serum (FBS). CD31$^+$/CD146$^-$ SP cells were cultured in EBM-2 with 10 ng/mL bFGF, 10 ng/mL vascular endothelial growth factor (VEGF), 138 nM hydrocortisone, 0.09 mg/mL heparin, 50 μg/mL ascorbic acid, and 10% FBS. They were routinely subcultured up to 70% confluence under identical conditions.

Cerebral ischemia model

All animal experiments were approved by the Institutional Animal Care and Use Committee (National Center for the Geriatrics and Gerontology). Adult male Sprague-Dawley rats (Japan SLC, Inc.) weighing 300–400 g were used. Animals were initially anesthetized with 5% isoflurane (Abbott Laboratories) and maintained under anesthesia with 1.5% isoflurane in a mixture of 70% N_2O and 30% O_2. Rectal

[1]Department of Oral Disease Research, National Center for Geriatrics and Gerontology, Research Institute, Obu, Aichi, Japan.
[2]Department of Oral and Maxillofacial Surgery, Laboratory Medicine, Nagoya University Graduate School of Medicine, Nagoya, Japan.
[3]Department of Vascular Dementia Research, National Center for Geriatrics and Gerontology, Research Institute, Obu, Aichi, Japan.

temperature was maintained at 37°C ± 0.5°C on a heating pad. Focal cerebral ischemia was induced by TMCAO with 2 h.[6] A 4-0 monofilament nylon suture (Shirakawa) with the tip rounded by flame heating and silicone (KE-200; Shin-Etsu Chemical) was advanced from the external carotid artery into the internal carotid artery until it blocked the origin of the MCA. Two hours after occlusion, reperfusion was performed by withdrawal of the suture. The regional cerebral blood flow of the MCA territory was measured using a laser-Doppler flowmeter (Omega FLO-N1; Omega Wave, Inc.) after occlusion. The response was considered positive and included only if the reduction in regional cerebral blood flow was >70%.

Transplantation

Twenty-four hours after TMCAO (day 0), the rats were again anesthetized with sodium pentobarbital (Schering-Plough) (0.25 mL/kg, intraperitoneally) and maintained under anesthesia with 1.5% isoflurane in a mixture of 70% N_2O and 30% O_2. Animals were randomly divided into three groups: (I) $CD31^-/CD146^-$ SP cell transplantation group ($n=24$, day 3 sacrificed = 6, day 9 sacrificed = 7, day 21 sacrificed = 11), (II) unfractionated pulp cell transplantation group ($n=4$, used for motor function), and (III) vehicle alone (phosphate-buffered saline [PBS]) group ($n=20$, day 3 sacrificed = 6, day 9 sacrificed = 5, day 21 sacrificed = 9). The infarction site was targeted for transplantation at the striatum of the following coordinates: 1.0 mm rostral to the bregma, 6.0 mm lateral to the midline, 5.0 mm ventral to the dura (Fig. 1A, B). Subsequently, 1×10^6 $CD31^-/CD146^-$ SP cells or unfractionated pulp cells at the fifth to seventh passage after labeling with 1,1-dioctadecyl-3,3,3,3 tetramethylindocarbocyanine perchlorate (DiI; Sigma), and removing all added factors into each medium were diluted with 2 μL of PBS, and were transplanted by Hamilton microsyringe (Hamilton). The control group consisted of an equal volume of PBS injected into the same site.

Immunohistochemistry

At day 3 or 21 after injection, the rat was transcardially perfused with 4% paraformaldehyde solution (Nakarai Tesque). The brain was removed and postfixed in paraformaldehyde. The following day, it was immersed in 30% sucrose solution. Twelve-micrometer-thick coronal sections were cut on a cryostat. For immunohistochemistry, the sections were preincubated in blocking solution (PBS containing 5% normal serum of the species in which the secondary antibody was raised) for 2 h at room temperature, and incubated with primary antibodies diluted for 1 h at room temperature. The primary antibodies were as follows: neuronal progenitor cells (NPC) marker, rabbit anti-doublecortin (1:50; Abcam, Inc.); neuron marker, rabbit anti-neurofilament H (1:200; Chemicon) and mouse anti-NeuN (anti-neuronal nuclei, 1:500; Chemicon); endothelial cell marker, mouse anti-RECA1 (rat endothelial cell antigen; Monosan); apoptosis marker, rabbit anti-cleaved caspase-3 (1:50; Cell Signaling Technology, Inc.); and VEGF marker, rabbit anti-VEGF (VEGF [P-20]: sc-1836; Santa Cruz Biotech). After washing, sections were incubated for 1 h at room temperature with secondary antibodies (on day 21, for neurofilament H/doublecortin, Donkey anti-rabbit IgG FITC [1:400; Jackson ImmunoResearch]; for NeuN/RECA1, Goat anti-mouse IgG FITC [1:200; MP Biomedicals]; and for VEGF, rabbit anti-goat IgG-HRP [1:400; Invitrogen Corporation]. On day 3, for cleaved caspase-3, goat anti-rabbit IgG-HRP [1:400; Invitrogen] and for VEGF, rabbit anti-goat IgG-HRP [1:400; Invitrogen]). The sections with HRP-conjugated secondary antibodies were incubated in anti-fluorescein-HRP (1:400; TSA™ Fluorescence Systems; PerkinElmer) for 7 min at room temperature. Adjacent sections were used as negative controls. In the control sections, all procedures were processed in the same manner except that the primary antibodies were omitted. To identify migration of NPC from SVZ, we observed the cryosections on days 9 and 21 with anti-doublecortin on fluorescence microscope (BZ-9000; Keyence) and BZ-HIC (Keyence).

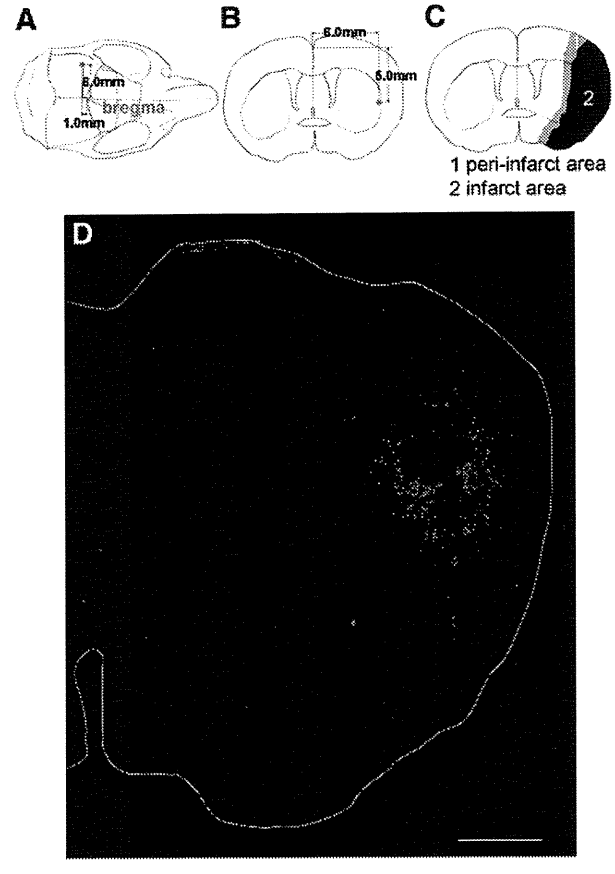

FIG. 1. **(A)** Overhead and **(B)** coronal view of the injection site. **(C)** The peri-infarct area. Peri-infarct area (gray), infarct core (black). **(D)** DiI-labeled transplanted $CD31^-/CD146^-$ SP cells (red) migrated from the original injection site to the peri-infarct area in the cortex and striatum. White outline is the outer circumference of brain. Scale bar = 1000 μm. SP, side population. DiI, 1,1-dioctadecyl-3,3,3,3 tetramethylindocarbocyanine perchlorate. Color images available online at www.liebertonline.com/tea

Statistical analyses of the density of cells

The density of NPCs, neurons, endothelial cells, and apoptotic cells in the peri-infarct area (Fig. 1C) and the contralateral region in the $CD31^-/CD146^-$ SP cell transplantation group and PBS groups were determined. In all groups (PBS group, $CD31^-/CD146^-$ SP cell transplantation group,

TABLE 1. PORCINE PRIMERS FOR REAL-TIME REVERSE TRANSCRIPTION–POLYMERASE CHAIN REACTION AND *IN SITU* HYBRIDIZATION

Gene		*5′ DNA sequence 3′*	*Product size (bp)*	*Accession no.*
r.β-actin	Forward	AAGTACCCCATTGAACACGG	257	NM_031144
	Reverse	ATCACAATGCCAGTGGTACG		
p.β-actin	Forward	CTGGGGCCTAACGTTCTCAC	198	BI118314
	Reverse	GTCCTTTCTTCCCCGATGTT		
VEGF	Forward	ATGGCAGAAGGAGACCAGAA	224	MN_214084
	Reverse	ATGGCGATGTTGAACTCCTA		
BDNF	Forward	TTCAAGAGGCCTGACATCGT	180	MN_214259
	Reverse	AGAAGAGGAGGCTCCAAAGG		
NGF	Forward	TGGTGTTGGGAGAGGTGAAT	210	L31889
	Reverse	CCGTGTCGATTCGGATAAA		
GDNF	Forward	ACGGCCATACACCTCAATGT	144	GU229658
	Reverse	CCGTCTGTTTTTGGACAGGT		

BDNF, brain-derived neurotrophic factor; GDNF, glial cell line-derived neurotrophic factor; NGF, nerve growth factor; VEGF, vascular endothelial growth factor.

and contralateral group, $n=3$), each five sections at every 120-μm were stained with doublecortin, NeuN, RECA1, and cleaved caspase-3. The microscopic images were scanned and five typical frames (0.49 mm^2) were measured for each section. Thus, 75 frames on an average were determined per group. The positively stained area relative to total area (7.41 mm^2) was statistically analyzed using a Dynamic cell count, BZ-HIC (Keyence).

Real-time reverse transcription–polymerase chain reaction

Total RNA on cryosamples was extracted using Trizol (Invitrogen) from the area of the DiI-positive cells observed in the section. First-strand cDNA syntheses were performed from total RNA by reverse transcription with ReverTra Ace-α (Toyobo). Real-time reverse transcription–polymerase chain reaction (RT-PCR) amplifications were performed at 95°C for 10 s, at 62°C for 15 s, and at 72°C for 8 s using the porcine-specific primers *VEGF*. The specificity of the primers to porcine was confirmed by no amplification of the first-strand cDNA from rats with normal brains. The RT-PCR products were subcloned into a pGEM-T Easy vector (Promega) and confirmed by DNA sequencing based on published cDNA sequences. Gene expression of the transplanted cells in the infarct area was compared with that in the porcine normal brain tissue and that in transplanted cells in the normal brain after normalizing with β-actin.

In situ *hybridization*

Neurotrophic factors expressed in $CD31^-/CD146^-$ SP cells were examined with *in situ* hybridization in cryosections on day 21. Porcine cDNA of *VEGF* (224 bp), glial cell line-derived neurotrophic factor (*GDNF*; 144 bp), brain-derived neurotrophic factor (*BDNF*;180 bp), and nerve growth factor (*NGF*; 210 bp) were linearized with *Nco*I, *Spe*I, *Nco*I, and *Spe*I, respectively, for anti-sense probes, and linearized with *Spe*I, *Nco*I, *Spe*I, and *Nco*I, respectively, for sense probes. The *VEGF* probe was constructed from plasmids after subcloning the PCR products using the same primers designed for real-time RT-PCR. The *GDNF*, *BDNF*, and *NGF* probes were also constructed in same way as the *VEGF* probe. Since a published porcine *GDNF* sequence was not available, human primers for *GDNF* (forward 5′-TATGGGATGTCGT GGCTGT-3′, reverse 5′-TCCACACCTTTTAGCGGAAT-3′) were used for cDNA subcloning of porcine *GDNF* (630 bp). The design of the oligonucleotide primers (Table 1) was based on both published porcine cDNA sequences and the newly cloned cDNA sequence of the porcine *GDNF*. The four probes were labeled with DIG (Invitrogen) and the DIG signals were detected with TSA system FITC-conjugated tyramide (Invitrogen).

Migration, proliferation, and anti-apoptotic assays

At 50% confluence, the culture medium was switched to serum-free EBM-2. The conditioned medium (CM) from $CD31^-/CD146^-$ SP cells, $CD31^+/CD146^-$ SP cells, and unfractionated pulp cells were collected after 48 h.

For migration assay, modified Boyden chamber assays were performed with polyethylene terephthalate membrane (BD Bioscience) in a 24-well plate (BD Bioscience). SHSY5Y cells (Sanyo Chemical Industries, Ltd.) (1×10^5 cells/well) were seeded on the insert polyethylene terephthalate membrane, and 500 μL of DMEM-F12 (Sigma) with 20% of the three CMs was, respectively, poured into the tissue culture 24-well plate. SHSY5Y cells were derived from a neural crest tumor of early childhood, predominantly composed of undifferentiated neuroblast-like cells.[7] After 24 h, the SHSY5Y cells passing through the membrane were counted after detaching them with 0.05% trypsin–0.02% EDTA.

For cell proliferation assay, SHSY5Y cells (1×10^3/96-well plate) were cultured in DMEM-F12 containing 10% FBS for 24 h, and subsequently in serum-free DMEM-F12 containing 0.2% bovine serum albumin for further 24 h. Then, the medium was changed into each DMEM-F12 containing 0.02% FBS with 20% of three CMs. Ten micrometers of Tetra-color one (Seikagaku Kogyo, Co.) was added to the 96 well-plate, and cell numbers were measured by spectrophotometry at 450 nm at 2, 12, 24, 36, and 48 h of culture.

For the anti-apoptotic assay, SHSY5Y cells were cultured in DMEM-F12 in a 35-mm dish for 2 days and then incubated with 300 nM staurosporine[8] (Sigma) in DMEM-F12 with 20% of the three CMs. After 24 h, SHSY5Y were harvested, and

the cell suspensions were treated with Annexin V-FITC (Roche Diagnostics) and PI for 15 min, and analyzed by flow cytometry JSAN.

BDNF (Peprotech), GDNF (Peprotech), VEGF-A (Peprotech), or NGF (Peprotech) at 50 ng/mL was used as a control for the three assays.

Evaluation of motor disability

Rats were blindly examined on days 0, 2, 6, and 9 with a standardized motor disability scale by slight modifications.[9] Rats were scored 1 point for each of the following parameters: flexion of the forelimb contralateral to the stroke when instantly hung by the tail, extension of the contralateral hind limb when pulled from the table, and rotation to the paretic side against resistance. In addition, 1 point was scored for circling motion to the paretic side when trying to walk, 1 point was scored for failure to walk out of a circle of 50 cm in diameter within 10 s, 2 points were scored for failure to leave the circle within 20 s, and 3 points were scored for inability to exit the circle within 60 s. In addition, 1 point each was scored for inability of the rat to extend the paretic forepaw when pushed against the table from above, laterally, and sideways. The motor disability scale was performed 3 times per animal time-point.

Assessment of infarct volume

The cryosections obtained from samples on days 3 and 21 were stained with hematoxylin and eosin.[10] ImageJ (National Institutes of Health) was used to determine each infarct area in 9 coronal sections in 12-μm thickness at 0.84-mm intervals. All of the infarction area was covered by these nine coronal sections. Regional infarct volumes were calculated by summing the infarct areas and multiplying these areas by the distance between sections (0.84 mm), followed by remediation for brain edema.[11]

Statistical analyses

Data are reported as means ± SD. p-Values were calculated using the unpaired Student's t-test.

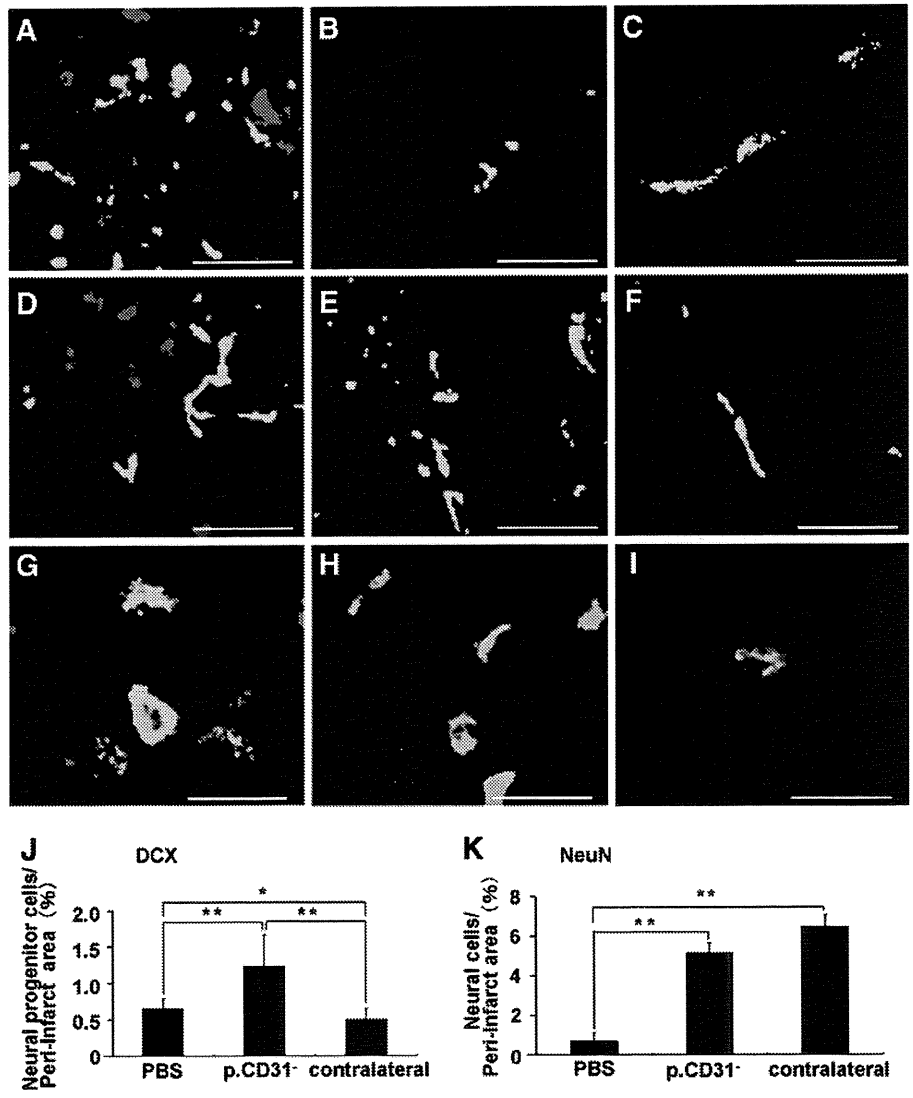

FIG. 2. Doublecortin-positive cells (green: **A–C**), Neurofilament-positive cells (green: **D–F**), and NeuN-positive cells (green: **G–I**). $CD31^-/CD146^-$ SP cells (red) transplantation group of the ipsilateral **(A, D, G)** and the contralateral **(B, E, H)** on day 21. PBS group **(C, F, I)** on day 21. Statistical analyses of density of NPCs **(J)** and neurons **(K)** on day 21. Scale bars = 20 μm. $*p < 0.005$, $**p < 0.001$, Student's t-test. Each point is expressed as mean ± SD of 75 determinations. NPC, neuronal progenitor cells; PBS, phosphate-buffered saline. Color images available online at www.liebertonline.com/tea

Results

Pulp stem cell outcome

DiI-labeled transplanted $CD31^-/CD146^-$ SP cells were characterized by round-to-oval nuclei with minimal variable cytoplasm. The transplanted cells survived and migrated from the original injection site to peri-infarct area in the cortex and striatum (Fig. 1D).

Transplanted cells localized in proximity of doublecortin (Fig. 2A) and neurofilament (Fig. 2D) or NeuN-positive cells (Fig. 2G) on day 21. Few doublecortin cells were observed in the contralateral side (Fig. 2B). There was a twofold increase in doublecortin-positive cells (Fig. 2J) and an eightfold increase in NeuN-positive cells (Fig. 2K) on day 21 in the $CD31^-/CD146^-$ SP cell transplantation group compared with that in the PBS group. No evidence of differentiation of $CD31^-/CD146^-$ SP cells into neurons or endothelial cells was detected. The migration of NPCs with doublecortin from SVZ to the peri-infarct area was observed on days 9 and 21. The migration on day 9 was more prominent (Fig. 3I, K, M). These results suggest that the transplanted cells support the migration and differentiation of the NPCs. The number of

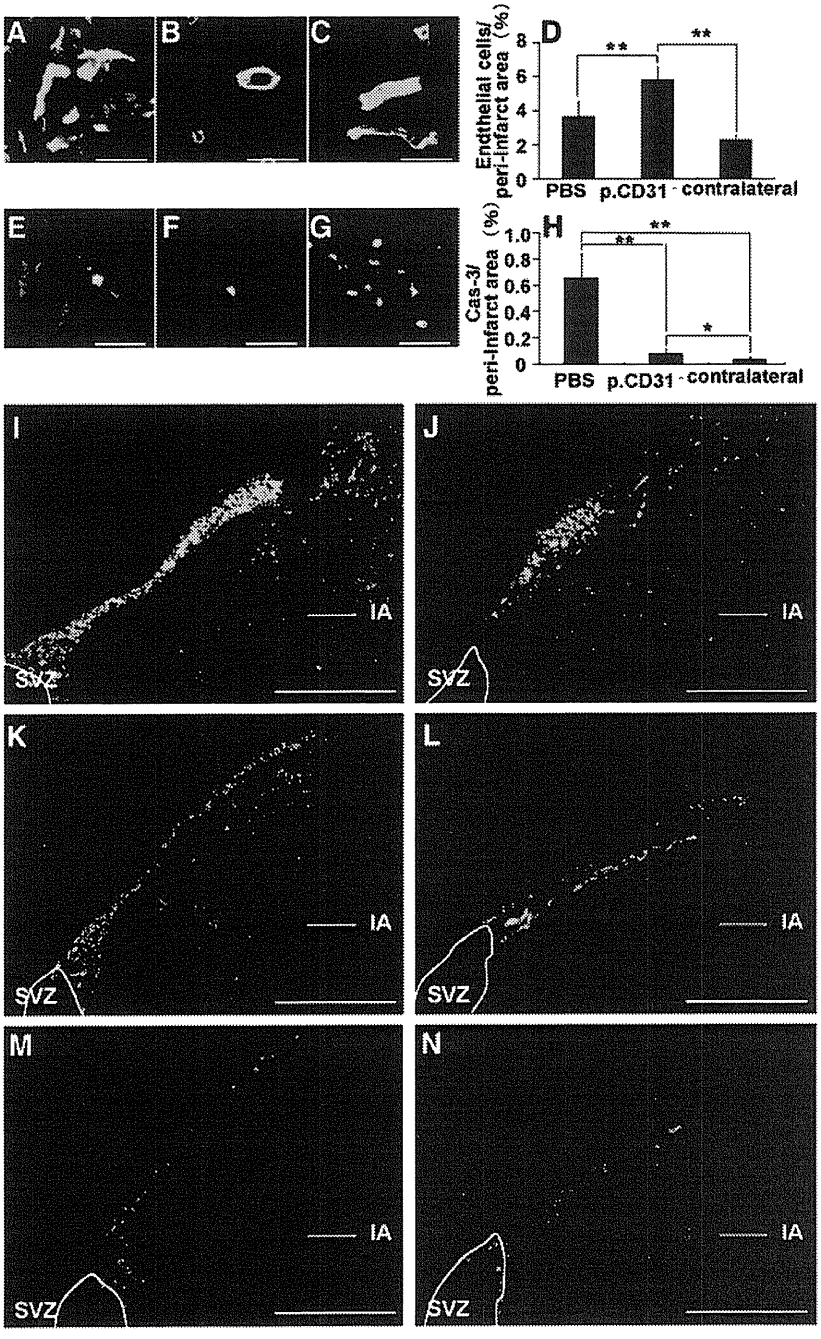

FIG. 3. RECA1-positive cells on day 21 (green: **A–C**) and cleaved caspase-3-positive cells on day 3 (green: **E–G**). $CD31^-/CD146^-$ SP cells (red) transplantation group of the ipsilateral **(A, E)** and the contralateral **(B, F)**. PBS group **(C, G)**. Statistical analyses of density of endothelial cells on day 21 **(D)** and cleaved caspase-3-positive cell on day 3 **(H)**. The migration of NPC from the SVZ to the peri-infarct area on days 9 **(I, J, M)** and 21 **(K, L, N)**. $CD31^-/CD146^-$ SP cells group **(I, J)**. Unfractionated pulp cells **(K, L)**. PBS group **(M, N)**. Scale bar = 20 μm **(A–C, E–G)**, and 300 μm **(I–N)**. $^*p < 0.01$, $^{**}p < 0.001$, Data were expressed as means ± SD at 75 determinations. The statistical difference was calculated by Student's *t*-test. IA, infarct area; SVZ, subventricular zone. Color images available online at www.liebertonline.com/tea

RECA1-positive cells on day 21 was increased in the CD31$^-$/CD146$^-$ SP cell transplantation group compared with that in the PBS group (Fig. 3D), indicating that the transplanted cells also promote angiogenesis after ischemia. In the CD31$^-$/CD146$^-$ SP cell transplantation group (Fig. 3H), there was a decrease in cleaved caspase-3-positive cells, suggesting that the transplanted cells have an anti-apoptotic function.

Expression of neurotrophic factors

The expression of several neurotrophic factors *VEGF*, *GDNF*, *NGF*, and *BDNF* was detected with *in situ* hybridization in the DiI-labeled CD31$^-$/CD146$^-$ SP cells in the peri-infarct area on day 21 (Fig. 4A–D). Real-time RT-PCR analysis demonstrated that expression of *VEGF* mRNA by the transplanted CD31$^-$/CD146$^-$ SP cells in the ischemic region on day 21 was 1,000 times and 28 times higher than that of normal porcine brain and that of the transplanted CD31$^-$/CD146$^-$ SP cells into normal rat striatum, respectively (Fig. 4E, F). Immunohistochemistry of VEGF showed that the VEGF protein was highly expressed in the DiI-labeled CD31$^-$/CD146$^-$ SP cells in the peri-infarct area on day 3 (Fig. 4G) compared with that on day 21 (Fig. 4H).

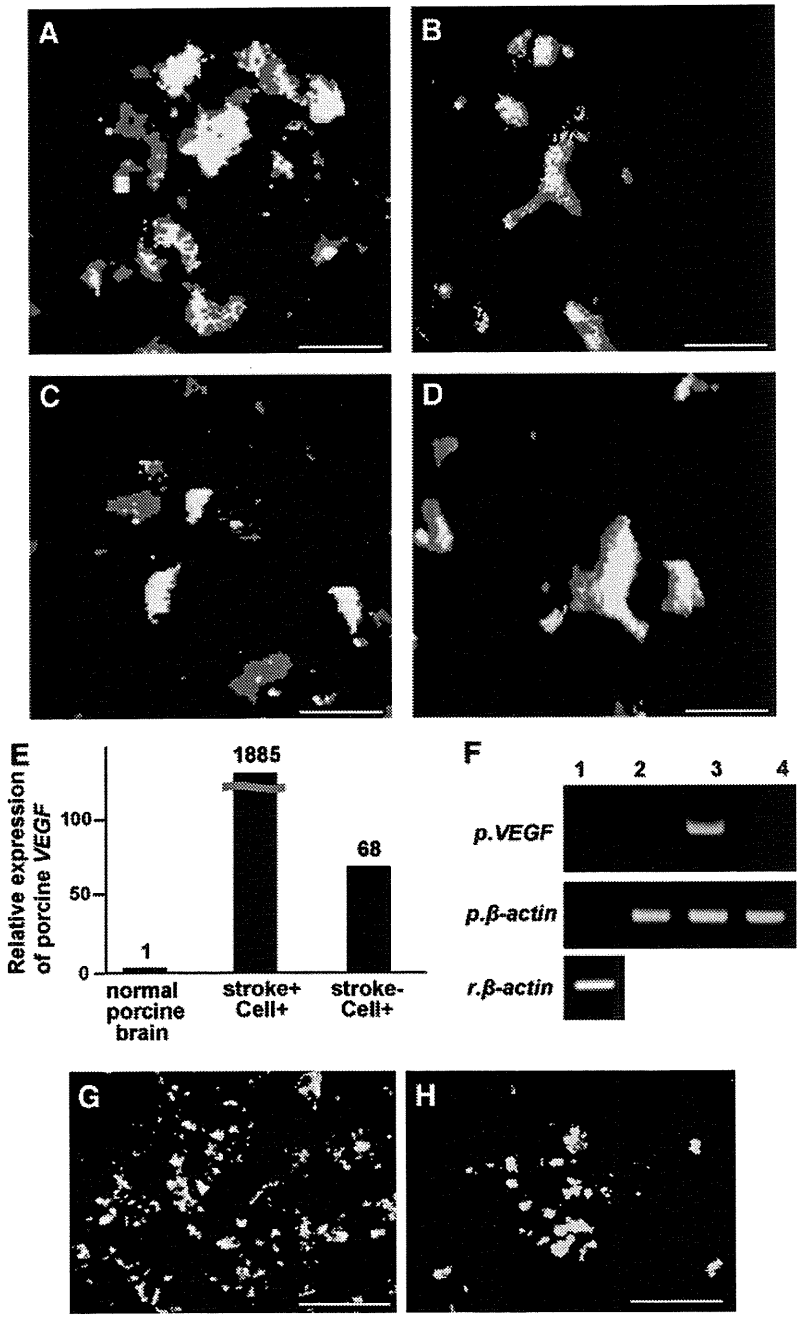

FIG. 4. Analysis of expression of *VEGF* **(A)**, *GDNF* **(B)**, *BDNF* **(C)**, and *NGF* **(D)** (green: **A–D)** of DiI-labeled transplanted CD31$^-$/CD146$^-$ SP cells (red) by *in situ* hybridization in the peri-infarct area. Real-time reverse transcription–polymerase chain reaction analysis of porcine *VEGF* (*pVEGF*) using porcine-specific primers **(E)**. Expression of porcine *VEGF* and porcine-specific and rat-specific β-actin 1, normal rat brain; 2, normal porcine brain; 3, peri-infarct area 21 days after transplantation of CD31$^-$/CD146$^-$ SP cells; 4, normal rat striatum 21 days after transplantation of the cells **(F)**. VEGF-positive cells on day 3 **(G)** and on day 21 **(H)** by immunohistochemistry. Scale bars = 10 μm **(A–D)** and 100 μm **(G, H)**. BDNF, brain-derived neurotrophic factor; GDNF, glial cell line-derived neurotrophic factor; NGF, nerve growth factor; VEGF, vascular endothelial growth factor. Color images available online at www.liebertonline.com/tea

Migration, proliferation, and anti-apoptotic assays

CM of CD31$^-$/CD146$^-$ SP cells showed higher migratory effect on SHSY5Y cells than VEGF, NGF, and BDNF, and was similar to GDNF (Fig. 5A). Its proliferation effect was higher than VEGF and NGF, and similar to BDNF and GDNF (Fig. 5B). Its anti-apoptotic activity was higher than BDNF, GDNF, and VEGF (Fig. 5C).

Evaluation of motor function

All groups (CD31$^-$/CD146$^-$ SP cells, unfractionated pulp cells, and PBS) displayed high score for motor function at the early stage (day 0, scores are 8.08±0.79; 8.25±0.96; 8.42±0.79, and day 2, 5.08±0.90; 6.25±1.26; 7.67±0.78, respectively). Progressive improvement in motor disability in the CD31$^-$/CD146$^-$ SP cell transplantation group after day 2 became significant on day 6 compared with PBS control group (2.67±1.23; 6.83±0.72), and more significant on day 9 compared with the unfractionated pulp cells and the PBS control group (1.33±0.78; 2.8±0.96; 6.50±0.67) (Fig. 6A). Persistent improvement in CD31$^-$/CD146$^-$ SP cells transplantation group was noted on day 14 (1.00±0.71) and 21 (0.80±0.45), whereas persistent impairment of motor disability (score above 4) was observed in the PBS group on day 14 (5.60±0.55) and 21 (5.40±0.59) (Fig. 6A). Further, the video image demonstrated significant recovery in motor function of the CD31$^-$/CD146$^-$ SP cell transplantation group compared with the unfractionated pulp cells and PBS control groups on day 6 (Supplementary Videos S1–S3; Supplementary Data are available online at www.liebertonline.com/tea).

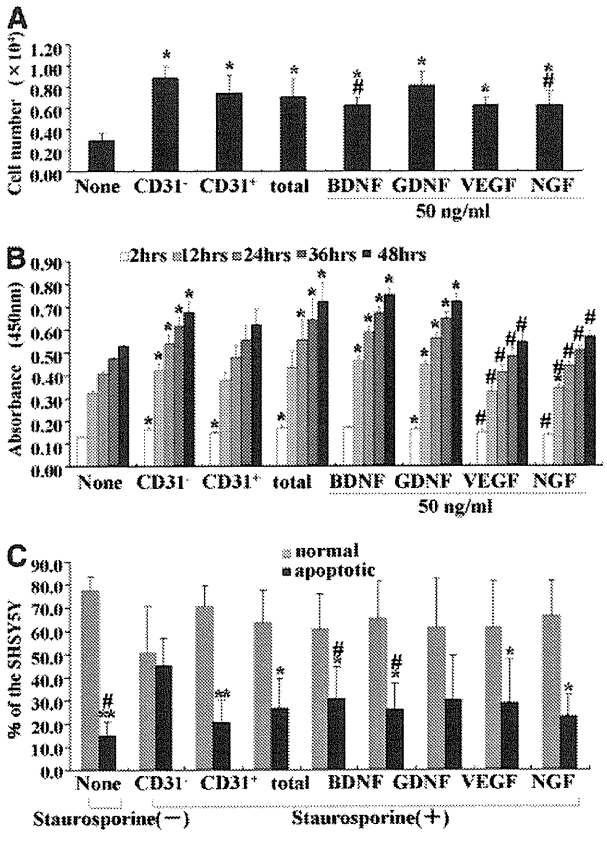

FIG. 5. The migration **(A)**, proliferative effect **(B)**, and anti-apoptotic effect **(C)** of conditioned medium of CD31$^-$/CD146$^-$ SP cells, CD31$^+$/CD146$^-$ SP cells, and unfractionated total pulp cells and neurotrophic factors on SHSY5Y cells. $^*p<0.05$, $^{**}p<0.005$, versus control. $^{\#}p<0.05$, versus CD31$^-$/CD146$^-$ SP cells. Data were expressed as means±SD at three determinations **(A, C)** and four determinations **(B)**. Student's *t*-test.

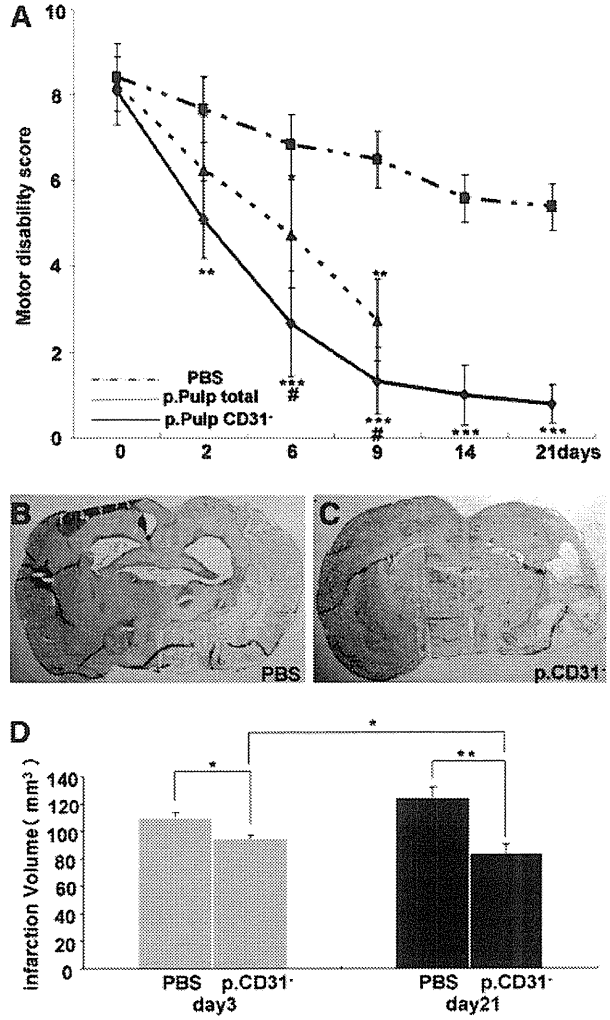

FIG. 6. Motor disability test by injection of the CD31$^-$/CD146$^-$ SP cells, the unfractionated pulp cells and the PBS on days 0, 2, 6, and 9 **(A)**. Infarct area on day 21 **(B, C)**. The reduction of the infarct volume 3 and 21 days after injection of CD31$^-$/CD146$^-$ SP cells **(D)**. $^*p<0.05$, $^{**}p<0.005$, $^{***}p<0.001$, versus control. $^{\#}p<0.05$, versus CD31$^-$/CD146$^-$ SP cells. Data were expressed as means±SD at three determinations **(D)**, Student's *t*-test.

Reduction of infarct volume

There was a significant decrease in the infarct volume on days 3 and 21 in the CD31$^-$/CD146$^-$ SP cell transplantation

group (day 3, $95.2 \pm 2.5\,mm^3$, $n=3$: day 21, $84.7 \pm 6.5\,mm^3$, $n=4$) compared to PBS group (day 3, $109.7 \pm 4.1\,mm^3$, $n=3$: day 21, $123.9 \pm 7.4\,mm^3$, $n=4$). The difference of infarct volume between the $CD31^-/CD146^-$ SP cell transplantation group and the PBS group increased over time (reduced by 13.3% on day 3 and reduced by 32.9% on day 21) (Fig. 6D). These results suggest that transplanted $CD31^-/CD146^-$ SP cells promoted the regeneration.

Discussion

In the current study, we demonstrated that transplanted $CD31^-/CD146^-$ SP cells migrated to the peri-infarct area. In addition, these cells released neurotrophic factors, and promoted migration and differentiation of the endogenous NPCs in SVZ. They also induced vasculogenesis in the peri-infarct area. These results indicate that $CD31^-/CD146^-$ SP cells ameliorated the ischemic tissue injury and accelerated the functional recovery after TMCAO. We have hypothesized that three mechanisms may contribute to the actions of VEGF. First, VEGF produced by transplanted cells may promote neurogenesis. NPCs in SVZ are known to migrate to the peri-infarct area and differentiate into neurons.[1] In this study, VEGF induced a chemotactic response in SHSY5Y cells. The transplanted $CD31^-/CD146^-$ SP cells migrated to the peri-infarct area and expressed VEGF. These results suggest that VEGF released by $CD31^-/CD146^-$ SP cells in the peri-infarct may promote migration of the endogenous NPCs in SVZ. Second, VEGF produced by transplanted cells may promote vasculogenesis. VEGF binds to its receptors on locally present vascular endothelial cells and directly initiates the angiogenic response.[12] In this study, the number of RECA1-positive endothelial cells significantly increased in the cell transplantation group. Third, VEGF may provide a neuroprotective effect. The neuroprotective effects of VEGF in experimental cerebral ischemia have been reported.[13] In cell the transplantation group, the number of cleaved caspase-3-immunopositive cells in the peri-infarct area was decreased compared with that in the PBS group, thus demonstrating the anti-apoptotic effects of VEGF on SHSY5Y cells. These results suggest that VEGF produced by $CD31^-/CD146^-$ SP cells may inhibit apoptosis of neurons. Thus, VEGF demonstrates pleiotropic effects on neurogenesis, vasculogenesis, and neuroprotection.

As VEGF is a potent vascular permeability factor, it may accelerate brain edema after stroke. Administration of VEGF in early ischemia (1 h after ischemia) leads to significant increase in blood–brain barrier leakage as well as enlarged ischemic areas.[14] However, VEGF administration at 24 h after TMCAO reduces infarct size, improves neurologic recovery, enhances neurogenesis in the SVZ and angiogenesis in the ischemic border zone.[14] In this study, $CD31^-/CD146^-$ SP cells were transplanted 24 h after TMCAO and we monitored the reduction of infarct size and improvement of motor disability. The time of administration of cells is critical. Thus, if $CD31^-/CD146^-$ SP cells were transplanted during an optimal window of time, they exhibit beneficial effects without the deleterious effects of edema.

In addition, $CD31^-/CD146^-$ SP cells expressed other neurotrophic factors such as GDNF,[15] NGF,[16] and *BDNF*[16] in the peri-infarct area. These neurotrophic factors had migratory, proliferative, and/or anti-apoptotic effects on SHSY5Y cells *in vitro* and may also contribute to the recovery from ischemic brain injury.

Finally, we explored the plausible underlying mechanisms of how injection of $CD31^-/CD146^-$ SP cells into the brains of immunocompetent rats staved off graft rejection. Blood–brain barrier is known to play a critical role in maintaining the immune-privileged status of the central nervous system.[17] It is well known that mesenchymal stem cells from bone marrow are not rejected by hosts and immunosuppression is not required in rodents.[1] Dental pulp stem cells have many similarities to mesenchymal stem cells; transplanted $CD31^-/CD146^-$ SP cells possess immunosuppressive properties.[18]

Conclusion

In summary, the transplantation of porcine $CD31^-/CD146^-$ SP cells promotes neurogenesis and vasculogenesis in an induced peri-infarct area, and enhances recovery after TMCAO in rats. Further research is needed to understand the underlying mechanisms. For potential clinical application and translational studies, the safety of $CD31^-/CD146^-$ SP cells must be assessed, including tumor formation. In conclusion, regeneration therapy using $CD31^-/CD146^-$ SP cells is a potential candidate in the treatment of stroke.

Acknowledgments

The authors thank Drs. Masataka Ito, Kayo Adachi, and Kiyomi Imabayasghi for their assistance. This work was supported by funds from Collaborative Development of Innovative Seeds, Potentiality verification stage from Japan Science and Technology Agency, a Grant-in-Aid for Scientific Research from the Ministry of Education, Science, Sports and Culture, Japan, No. 19659499 (M.N.), No. 20390504 (M.N.), and No. 18592173 (H.H.), and the Research Grant for Longevity Sciences (19C-2, 21A-7) from the Ministry of Health, Labour, and Welfare (M.N.).

Disclosure Statement

No competing financial interests exist.

References

1. Burns, T.C., Verfaillie C.M., and Low W.C. Stem cells for ischemic brain injury: a critical review. J Comp Neurol **515,** 125, 2009.
2. Locatelli, F., Bersano, A., Ballabio, E., Lanfranconi, S., Papadimitriou, D., Strazzer, S., Bresolin, N., Comi, G.P., and Corti, S. Stem cell therapy in stroke. Cell Mol Life Sci **66,** 757, 2009.
3. Gage, F.H., Kempermann, G., Palmer, T.D., Peterson, D.A., and Ray, J. Multipotent progenitor cells in the adult dentate gyrus. J Neurobiol **36,** 249, 1998.
4. Yang, K.L., Chen, M.F., Liao, C.H., Pang, C.Y., and Lin, P.Y. A simple and efficient method for generating Nurr1-positive neuronal stem cells from human wisdom teeth (tNSC) and the potential of tNSC for stroke therapy. Cytotherapy **11,** 606, 2009.
5. Iohara, K., Zheng, L., Wake, H., Ito, M., Nabekura, J., Wakita, H., Nakamura, H., Into, T., Matsushita, K., and Nakashima, M. A novel stem cell source for vasculogenesis in ischemia: subfraction of side population cells from dental pulp. Stem Cells **26,** 2408, 2008.

6. Longa, E.Z., Weinstein, P.R., Carlson, S., and Cummins, R. Reversible middle cerebral artery occlusion without craniectomy in rats. Stroke **20,** 84, 1989.
7. Koning, G., Colin, L., and Beyreuther, K. Retionic acid induced differentiated neuroblastoma cells show increased expression of the βA4 amyloid gene of Alzheimer's disease and an altered splicing pattern. FEBS Lett **269,** 305, 1990.
8. Richard, B., Eric, S., Patrick, O., Kurt, W., and Ywes, P. Induction of a common pathway of apoptosis by staurosporine. Exp Cell Res **211,** 314, 1994.
9. Leker, R.R., Gai, N., Mechoulam, R., and Ovadia, H. Drug-induced hypothermia reduces ischemic damage: effects of the cannabinoid HU-210. Stroke **34,** 2000, 2003.
10. Ginsberg, M.D. Adventures in the pathophysiology of brain ischemia: penumbra, gene expression, neuroprotection: the 2002 Thomas Willis Lecture. Stroke **34,** 214, 2003.
11. Leach, M.J., Swan, J.H., Eisenthal, D., Dopson, M., and Nobbs, M. BW619C89, a glutamate release inhibitor, protects against focal cerebral ischemic damage. Stroke **24,** 1063, 1993.
12. Plate, K.H., Beck, H., Danner, S., Allegrini, P.R., and Wiessner, C. Cell type specific upregulation of vascular endothelial growth factor in an MCA-occlusion model of cerebral infarct. J Neuropathol Exp Neurol **58,** 654, 1999.
13. Jin, K.L., Mao, X.O., and Greenberg, D.A. Vascular endothelial growth factor: direct neuroprotective effect in *in vitro* ischemia. Proc Natl Acad Sci U S A **97,** 10242, 2000.
14. Heike, B., and Karl, H.P. Angiogenesis after cerebral ischemia. Acta Neuropathol **117,** 481, 2009.
15. Leu-Fen, H., Lin, H., Doherty, D., Lile, B., and Frank, C. GDNF: a glial cell line-derived neurotrophic factor for midbrain dopaminergic neurons. Science **260,** 1072, 1993.
16. Shawne, N., Fernando, G., James, C., and Carl, C. Physical activity increases mRNA for brain-derived neurotrophic factor and nerve growth factor in rat brain. Brain Res **726,** 49, 1996.
17. Pachter, J.S., De Vries, H.E., and Fabry, Z. The blood-brain barrier and its role in immune privilege in the central nervous system. J Neuropathol Exp Neurol **62,** 593, 2003.
18. Pierdomenico, L., Bonsi, L., Calvitti, M., Rondelli, D., Arpinati, M., Chirumbolo, G., Becchetti, E., Marchionni, C., Alviano, F., Fossati, V., Staffolani, N., Franchina, M., Grossi, A., and Bagnara, G.P. Multipotent mesenchymal stem cells with immunosuppressive activity can be easily isolated from dental pulp. Transplantation **80,** 836, 2005.

Address correspondence to:
Misako Nakashima, Ph.D.
Department of Oral Disease Research
National Center for Geriatrics and Gerontology
Research Institute
35 Gengo, Morioka, Obu
Aichi 474-8522
Japan

E-mail: misako@ncgg.go.jp

Received: May 24, 2010
Accepted: January 10, 2011
Online Publication Date: February 22, 2011

Acceleration of Wound Healing with Stem Cell–Derived Growth Factors

Masayuki Tamari, DDS[1]/Yudai Nishino, DDS, PhD[2]/Noriyuki Yamamoto, DDS, PhD[3]/Minoru Ueda, DDS, PhD[4]

Purpose: *Recently, it has been revealed that bone marrow–derived mesenchymal stem cells (MSCs) accelerate the healing of skin wounds. Although the proliferative capacity of MSCs decreases with age, MSCs secrete many growth factors. The present study examined the effect of mesenchymal stem cell–conditioned medium (MSC-CM) on wound healing.* ***Materials and Methods:*** *The wound-healing process was observed macroscopically and histologically using an excisional wound-splinting mouse model, and the expression level of hyaluronic acid related to the wound healing process was observed to evaluate the wound-healing effects of MSC, MSC-CM, and control (phosphate-buffered saline).* ***Results:*** *The MSC and MSC-CM treatments accelerated wound healing versus the control group. At 7 days after administration, epithelialization was accelerated, thick connective tissue had formed in the skin defect area, and the wound area was reduced in the MSC and MSC-CM groups versus the control group. At 14 days, infiltration of inflammatory cells was decreased versus 7 days, and the wounds were closed in the MSC and MSC-CM groups, while a portion of epithelium was observed in the control group. At 7 and 14 days, the MSC and MSC-CM groups expressed significantly higher levels of hyaluronic acid versus the control group (P < .05). The expression level of hyaluronic acid was lower at 14 days than at 7 days in all three groups.* ***Conclusions:*** *Both the MSC and MSC-CM groups accelerated wound healing versus the control group to a similar degree. Accordingly, it is suggested that the MSC-CM contains growth factor derived from stem cells, is able to accelerate wound healing as well as stem cell transplantation, and may become a new therapeutic method for wound healing in the future.* ORAL CRANIOFAC TISSUE ENG 2011;1:181–187

Key words: *cell therapy, human mesenchymal stromal cell, hyaluronic acid, stem cell–derived growth factor, wound healing*

An intractable chronic wound exerts considerable stress on patients, and treatment of such wounds is very difficult.[1,2] Surgery and medical treatments have been performed to treat such wounds. However, there are many problems, including failure of wound healing and scarring, with these treatments. In addition, wound closure and treatment effectiveness cannot be guaranteed in many cases.[3] Therefore, effective treatment measures must be established. Many therapeutic approaches, including ointments, artificial skin, and substitute skin, have been developed. Furthermore, cell therapy, which is a low-aggression method to promote scar-free wound healing, has been explored. Many reports have demonstrated that the differentiation and paracrine effects of mesenchymal stem cells (MSCs) accelerate wound healing.[4–6] MSCs are referred to as stromal progenitor, self-renewing, and expandable stem cells and are able to differentiate into osteoblasts, adipocytes, chondrocytes, and other cell types.[7] However, bone marrow aspiration is invasive,

[1]Graduate student, Department of Oral and Maxillofacial Surgery, Nagoya University Graduate School of Medicine, Nagoya, Japan.
[2]Postdoctoral researcher, Department of Oral and Maxillofacial Surgery, Nagoya University Graduate School of Medicine, Nagoya, Japan.
[3]Assistant Professor, Department of Oral and Maxillofacial Surgery, Nagoya University Graduate School of Medicine, Nagoya, Japan.
[4]Professor, Department of Oral and Maxillofacial Surgery, Nagoya University Graduate School of Medicine, Nagoya, Japan.

Correspondence to: Dr Noriyuki Yamamoto, Department of Oral and Maxillofacial Surgery, Nagoya University Graduate School of Medicine, 65 Tsurumai-Cho, Showa-ku, Nagoya 466-8550 Japan. Fax: +81-52-744-2352. Email: noriyuki@med.nagoya-u.ac.jp